SEDIMENTOLOGY the journal of the International Association of Sedimentologists

Sedimentology (2020) **67**, 534–558 doi: 10.1111/sed.12653

Are carbonate barrier islands mobile? Insights from a mid to late-Holocene system, Al Ruwais, northern Qatar

JOHN RIVERS*, MAX ENGEL†‡, ROBERT DALRYMPLE§, RUQAIYA YOUSIF*, CHRISTIAN J. STROHMENGER¶ and ISMAIL AL-SHAIKH*

**Qatar Center for Coastal Research (QCCR), ExxonMobil Research Qatar, P.O. Box 22500, Qatar Science and Technology Park-Tech, Doha, Qatar (E-mail:John.m.rivers@exxonmobil.com)*

†Royal Belgian Institute of Natural Sciences, Geological Survey of Belgium, Jennerstraat 13, 1000 Brussels, Belgium

‡Institute of Geography, University of Cologne, Zülpicher Str. 45, 50674 Cologne, Germany

§Department of Geological Sciences and Geological Engineering, Queen's University, Miller Hall, 36 Union Street, Kingston, ON, K7L 3N6, Canada

¶ExxonMobil Upstream Integrated Solutions, 22777 Springwoods Village Parkway, Spring, TX, 77389, USA

Associate Editor – Stephen Lokier

ABSTRACT

Barrier islands are important landforms in many coastal systems around the globe. Studies of modern barrier island systems are mostly limited to those of siliciclastic realms, where the islands are recognized as mobile features that form on transgressive coastlines and migrate landward as sea-level rises. Barrier islands of the 'Great Pearl Bank' along the United Arab Emirates coast are the best-known carbonate examples. These Holocene islands, however, are interpreted to be anchored by older deposits and immobile. The mid-Holocene to late-Holocene depositional system at Al Ruwais, northern Qatar, provides an example of a mobile carbonate barrier island system, perhaps more similar to siliciclastic equivalents. Sedimentological and petrographic analyses, as well as ^{14}C-dating of shells and biogenic remains from vibracored sediments and surface deposits, show that after 7000 years ago a barrier system with a narrow back-barrier lagoon formed along what is now an exposed coastal zone, while, contemporaneously, a laterally-extensive coral reef was forming immediately offshore. After 1400 years ago the barrier system was forced to step *ca* 3 km seaward in response to a sea-level fall of less than 2 m, where it re-established itself directly on the mid-Holocene reef. Since that time, the barrier has retreated landward as much as 1000 m to its current position, exposing previously-deposited back-barrier lagoonal sediment at the open-coast shoreline. In modern neritic warm-water carbonate settings mobile barrier island systems are rare. Their construction and migration may be inhibited by reef formation, early cementation, and the relative inefficiency of sourcing beach sediments from open carbonate shelves. Carbonate barrier island systems likely formed more commonly during geological periods when ramps and unrimmed shelves predominated and in calcite seas, when meteoric cementation was minimized as a result of initial calcitic allochem mineralogy. As with their siliciclastic analogues, however, recognition of the influence of these transient landforms in the rock record is challenging.

Keywords Arabian Gulf, barrier island, carbonate ramp, Persian Gulf, sequence stratigraphy.

INTRODUCTION

Siliciclastic barrier island systems and the processes leading to their formation and migration have garnered significant attention over the past 45 years (Swift, 1975; Barwis & Hayes, 1979; Schwartz, 1982; Davis, 1985, 1994; Dalrymple *et al.*, 1992; Cooper *et al.*, 2012; Fruergaard *et al.*, 2015a,b, 2018; Kinsela *et al.*, 2016; Zaremba *et al.*, 2016; Oliver *et al.*, 2017a,b; Dougherty, 2018; Raff *et al.*, 2018). The barrier island model is widely applied to explain deposits observed along transgressive wave-dominated shorelines (Boyd, 2010), where the islands are interpreted to migrate landward with sea-level rise (e.g. Swift, 1975; Cowell *et al.*, 1999). Factors understood to influence the existence of siliciclastic barrier islands include the presence of: (i) sufficient wave energy to redistribute sand along the shoreline, although barrier island systems typically do not form when wave heights exceed 2 m (Flemming, 2012); (ii) tidal ranges of <3·5 m (Hayes, 1979), above which tidal currents counteract the influence of wave energy; as well as (iii) sufficient mobile sediment to build a barrier; (iv) a transport system to move sediment to the area of barrier formation; and (v) a low-gradient profile to provide space for a back-barrier lagoon to form (Davis, 1994). Although modern-day siliciclastic barrier island systems are common, occupying 12 to 13% of the world's shorelines (Pilkey & Fraser, 2003), equivalent carbonate barrier island systems are not abundant, comprising only 1% of all coasts (Stutz & Pilkey, 2001).

In the carbonate realm, on rimmed shelves and on shallow isolated platforms, significant linear grainstone bodies are generally observed in high-energy settings at seaward margins (Jones, 2010; Harris *et al.*, 2011), at locations where the tidal wave passes abruptly into shallow water and tidal current speeds reach maximum values (cf. Reynaud & Dalrymple, 2012, fig. 13·3). The location of these sand bodies (or shoals) are therefore dictated by the seaward extent of the underlying shelf or platform, and such deposits are not thought to migrate considerable distances from their marginal positions because of their genetic linkage with tidal-current amplification at that location. On unrimmed, shallow, warm-water carbonate shelves, such as are observed in the Gulf of Mexico (e.g. Logan *et al.*, 1969; Ginsburg & James, 1974), barrier islands are mostly absent. A notable exception is reported by Phleger & Ayala-Castanares (1971); however, the extent to which this example migrated landward during the post-glacial transgression is uncertain. Barrier island systems appear to be common along the shorelines of cool-water carbonate shelves of Australia, including the Coorong region of southeastern Australia (James & Bone, 2017; Joury *et al.*, 2018). With respect to carbonate ramps, the carbonate islands of the 'Great Pearl Bank' in the modern Arabian Gulf ramp setting are not considered similar to siliciclastic barrier islands, because they are thought to have formed on Pleistocene palaeo-topographic highs and are not interpreted as mobile (Purser & Evans, 1973). Shallow carbonate ramp systems are understood to have been more common in the geological past, including during greenhouse periods (Burchette & Wright, 1992). Depositional models of these ancient systems commonly indicate that high-energy shallow water sites, where waves impinge and barrier islands might form, were instead occupied by subaqueous 'shoals' (e.g. Calvet *et al.*, 1990; Seyedmehdi *et al.*, 2016), or depositional sand bodies referred to as 'ramp crests' (e.g. Kerans & Kempter, 2002). Although the possibility of carbonate barrier islands (or 'beach barriers') has been raised (Tucker & Wright, 1990; Tucker, 1991), their presence is not widely considered in carbonate sedimentological literature.

A carbonate barrier island system formed during the mid-Holocene to late-Holocene at the northern tip of the Qatar peninsula, near Al Ruwais (Purkis *et al.*, 2017). These Holocene deposits sit directly above dolomitized Eocene bedrock, allowing clear delineation of Holocene deposition from the ancient. The purpose of this contribution is to document this example and provide a model for how such carbonate island systems might have evolved in the ancient past. Critically, this study permits comparison of carbonate barrier islands with siliciclastic equivalents, offering insights as to why carbonate barrier islands are relatively less common in modern coastal systems, and whether this was also likely the case in past geological ages.

STUDY AREA

The Arabian Gulf is a foreland basin that sits at the southern foot of the Zagros Mountain range, an Eocene to recent orogen associated with collision of the Arabian and Eurasian plates (Dewey *et al.*, 1973; Glennie *et al.*, 1990; Marzouk & El

Sattar, 1994) (Fig. 1A). The basin is *ca* 800 km in length, 250 km wide and is mostly <60 metres water depth (mwd). Qatar is located in the southern portion of the Gulf (Fig. 1B), which is bathed in waters of <40 m depth and is the site of extensive carbonate sedimentation (Purser, 1973; Alsharhan & Kendall, 2003). The slope of the basin from the southern shallows to the deeper northern area is generally <2°, and the setting is described as a carbonate ramp (Ahr, 1973; Read, 1985), although this is not without caveats (Walkden & Williams, 1998).

During the last glacial maximum (LGM), which occurred about 18 ka, sea-level was *ca* 120 m lower than today (Fairbridge, 1961; Sarnthein, 1972; Kassler, 1973; Lambeck, 1996). At this time, the entire Arabian Gulf was exposed. The Gulf started to flood 14 ka (Lambeck, 1996) and sea-level rose close to that of the present-day coastline 7 to 6 ka. Shortly after 6 ka, the Holocene sea-level reached a highstand about 1·5 to 4·0 m above the present-day level (Kassler, 1973; Lambeck, 1996; Strohmenger *et al.*, 2010; Engel & Brückner, 2014; Lokier *et al.*, 2015) (Fig. 2). Between the present-day and 6 ka, sea-level has fallen to its current position (Strohmenger & Jameson, 2015), ultimately as a result of global seawater redistribution associated with hydroisostatic subsidence at continental margins (Mitrovica & Milne, 2002).

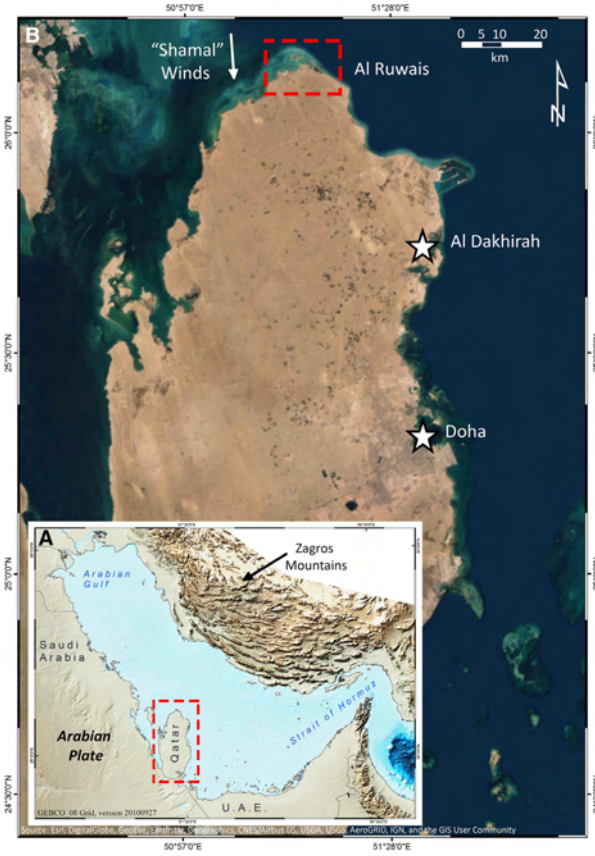

Fig. 1. (A) Location of Qatar (red rectangle) showing major tectonic and basinal features. (B) Satellite image of Qatar showing study area location (red rectangle) and dominant wind direction.

The Arabian Gulf is a semi-restricted body of water, connected to the Indian Ocean through the narrow Strait of Hormuz (Fig. 1A). The arid to hyper-arid continental subtropical climate of Qatar (Eccleston *et al.*, 1981; Glennie, 2005) reflects that of the region, and evaporation of gulf water greatly exceeds freshwater input (Kämpf & Sadrinasab, 2005; Sheppard *et al.*, 2010). Salinities are elevated throughout the Gulf for much of the year (Purser, 1973; Alsharhan & Kendall, 2003), and in the southern Gulf salinities commonly reach highs of >40 ppt in summer. Sea surface temperatures in the region generally fluctuate between 20°C and 28°C (Kämpf & Sadrinasab, 2005; Sheppard *et al.*, 2010). The dominant winds are the north-westerly 'shamal' winds which reach peak strengths in the late spring and summer (Fig. 1B) (Yu *et al.*, 2016). Whereas peak wind speeds can reach storm force, most windstorms are short and do not produce large ocean waves. Peak wave heights at the northern, windward coast seldom exceed 0·5 m (Loughland *et al.*, 2012). Storm surges are generally small, with amplitudes generally 1 m or less in the study area (El-Sabh & Murty, 1989). The coastlines of Qatar are affected by a semi-diurnal tide with a range of 1·1 to 2·3 m (Al-Yousef, 2003).

The carbonate depositional system offshore at Al Ruwais, has been documented in detail by Purkis *et al.* (2017) (Fig. 2). The coastal system is described as an inner-ramp [above fair-weather wave base (FWWB)] and proximal mid-ramp (below FWWB) carbonate realm. The most prominent depositional features in the study area are barrier islands (Jazeerat Reken and Umm Tays; Fig. 2) that further segregate the inner ramp into open and restricted settings. Northward, towards the open Gulf, barrier island beaches are composed of coarse to very coarse carbonate sands rich in red algal and coral remains. These sediments are sourced from moribund reefs or from their genetically-related sand sheets, which may be found immediately seaward of the islands. Immediately landward of the barrier-island-beaches, 2 m high coastal dune deposits are present, stabilized by low

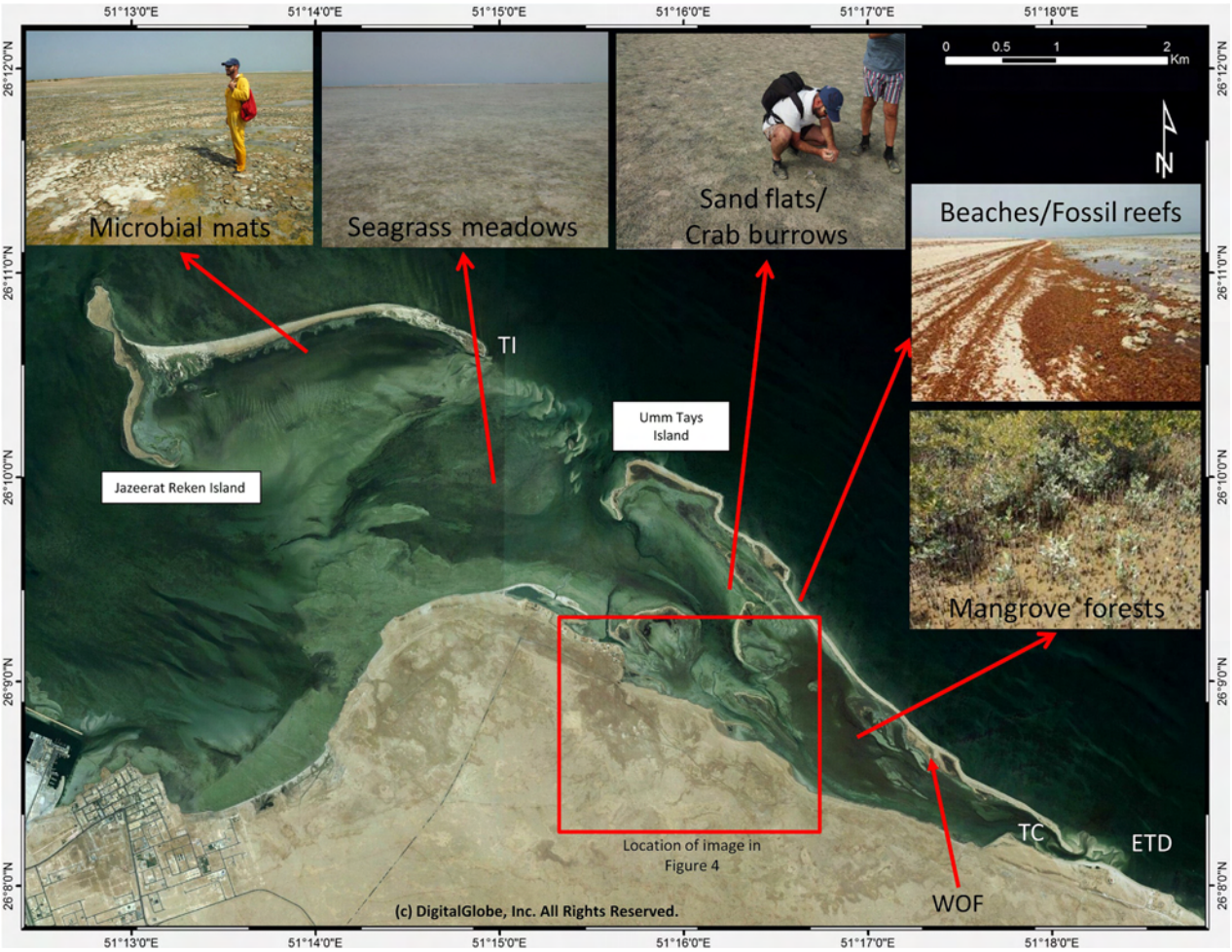

Fig. 2. WorldView-2 (2015) satellite image of the Al Ruwais region showing island names, components of the modern depositional system, and the location of Fig. 4. ETD, ebb-tide delta; TC, tidal channel; TI, tidal inlet; WOF, washover fan.

shrubs. These elevated features descend southward (landward) to crab-burrowed sand flats (with small amounts of carbonate mud) variably occupied by microbial mats (Fig. 2) that form in the protected upper intertidal settings directly behind the aeolian dunes. The open deeper intertidal and shallow subtidal lagoonal settings behind the barriers host fine-grained to medium-grained peloidal sand sheets, cut by tidal channels and irregularly populated by seagrass. Mangrove forests dissected by tidal creeks generally inhabit more restricted deeper intertidal and shallow subtidal areas behind Umm Tays Island.

Recent lithified and unlithified sediments can be observed at various locations along the low-lying (<4 m above sea-level) coastlines of Qatar, representing the mid-Holocene (2 to 7 ka) highstand (e.g. Billeaud *et al.*, 2014; Strohmenger & Jameson, 2015). Deposits of this age lie between the modern sediments described above, and the underlying Eocene bedrock that is exposed further inland. Similar highstand deposits can also be observed in the Al Ruwais region, onshore and directly landward of the active barrier-lagoon system. This study focuses on mapping and characterization of these mid-Holocene onshore rocks and sediments, and seaward deposits of equivalent age underlying the modern system and integrating this with information about the evolution of the modern barrier.

METHODS

Mid-Holocene to late-Holocene deposits were described using surface observations as well as trenching ($n = 1$) and vibracoring ($n = 7$) to a depth of up to 4 m below the ground surface.

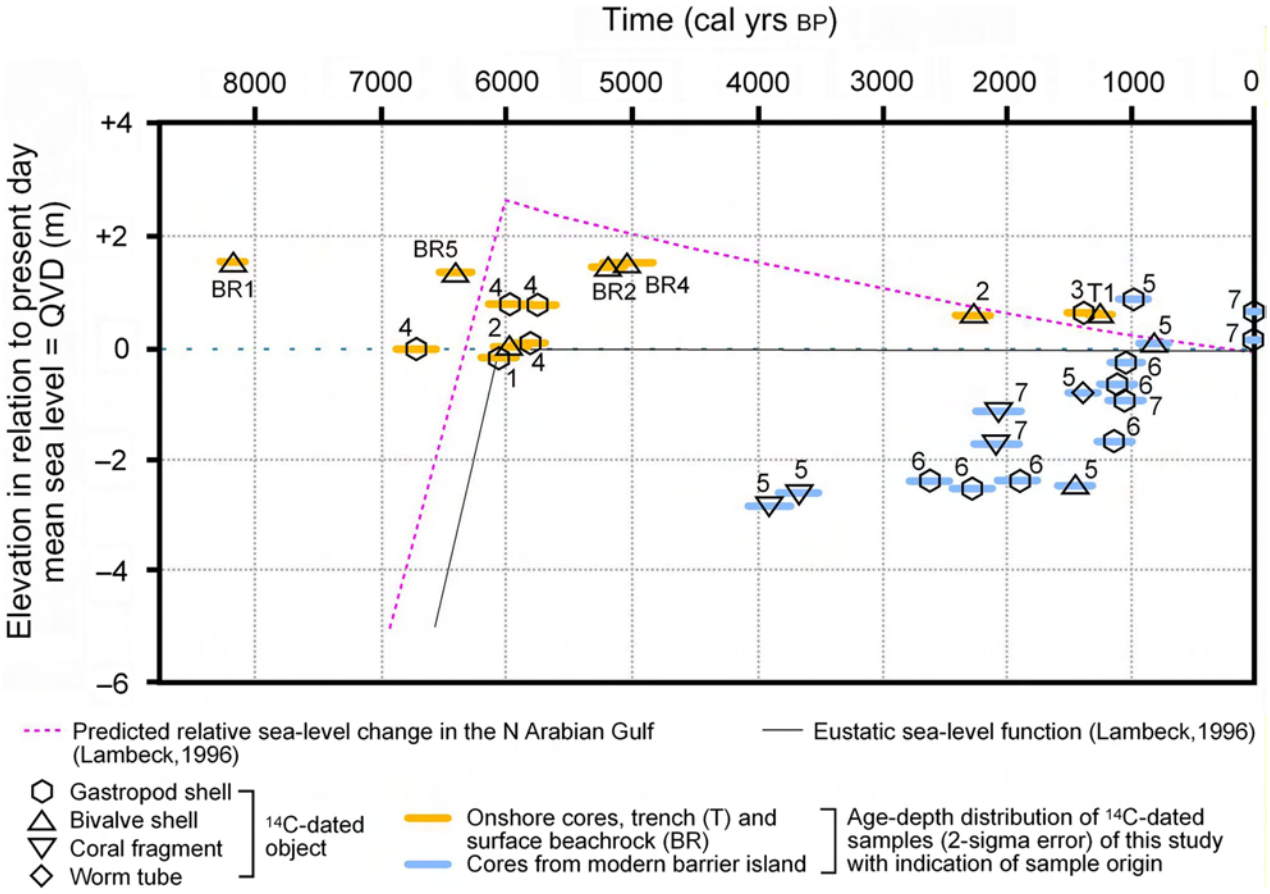

Fig. 3. Sea-level curve of Lambeck (1996) for the Arabian Gulf. ^{14}C age dates of allochems from both surface and core samples for this study are also plotted relative to sample elevation (Table 1). QVD refers to Qatar National Vertical Datum.

Vibracores were taken using an Atlas Copco hammer corer (Atlas Copco Limited, Hemel Hampstead, UK) using half-open steel probes with a diameter of 6·0, 5·0 or 3·6 cm. Cores and trenches were photographed and initially described in the field. The elevation of all sites was determined using a Topcon HiPer Pro differential global positioning system (DGPS) (Topcon Corporation, Tokyo, Japan). The measured grids were tied to cadastral survey points resulting in a lateral and vertical measurement error of ±2 cm (Table 1). Sedimentary components and Dunham's texture classifications (Dunham, 1962) were confirmed on selected samples using binocular microscopy as well as plane and polarized light microscopy of standard petrographic thin sections, half of each being stained with alizarin red-S to allow differentiation of calcite and aragonite. Because the deposits under study include both lithified and unlithified sediments, the Dunham texture classification is used for both. For simplicity, however, grainstone-textured unlithified sediments are commonly referred to as 'sands'.

Selected individual well-preserved and cement-free mollusc shells, worm tubes or coral fragments from the surface and shallow subsurface (n = 33) were cleaned with ethanol and deionized water and sent to Beta Analytic (Miami, FL, USA) for ^{14}C dating. All ages are reported as calibrated ages in calendar years before 1950 CE. For calibration the Marine13 calibration dataset was used (Reimer *et al.*, 2013) and a local ΔR value of 180 ± 53 years (Southon *et al.*, 2002) was applied. Samples selected for dating were not in life position with the notable exception of some coral samples (Table 1). Ages are plotted as a function of sample elevation and shown relative to the mid-Holocene to late-Holocene sea-level curve on Fig. 3. For mapping purposes, SPOT-5 (2·5 m resolution) and WorldView-2 (0·5 m resolution) satellite imagery were acquired.

Table 1. Location, elevation, depth, fossil type and measured age of ^{14}C dated samples.

Sample	Source	Latitude (*N*)	Longitude (E)	Elevation (m)	Sample depth (m)	Fossil type	Age (BP)
BR-1	Onshore Outcrop	26°9′0·7400″	51°15′34·3800″	1·44	Surface	Bivalve	8170 ± 100
BR-2	Onshore Outcrop	26°9′0·3900″	51°15′37·5300″	1·44	Surface	Bivalve	5180 ± 150
BR-3	Onshore Outcrop	26°8′56·9700″	51°15′58·0800″	NA	Surface	Bivalve	3410 ± 60
BR-4	Onshore Outcrop	26°8′43·8200″	51°16′23·8900″	1·53	Surface	Bivalve	5040 ± 200
BR-5	Onshore Outcrop	26°8′27·5600″	51°16′50·6500″	1·32	Surface	Bivalve	6400 ± 1230
CT1	Top Coral Terrace	26°9′51·00″	51°16′13·87″	NA	Surface	Coral*	1510 ± 50
CT2	Top Coral Terrace	26°9′51·00″	51°16′13·87″	NA	Surface	Coral*	1460 ± 90
T1-1	Trench 1	26°9′3·4482″	51°15′28·3032″	0·95	0·30	Bivalve	1250 ± 110
C1-1	Core 1	26°8′57·7788″	51°15′27·7164″	0·86	0·73	Gastropod	5810 ± 120
C2-1	Core 2	26°8′33·1100″	51°16′19·8600″	NA	0·85	Bivalve	5975 ± 140
C2-2	Core 2	26°8′33·1100″	51°16′19·8600″	NA	0·28	Bivalve	2265 ± 140
C3-1	Core 3	26°8′39·5052″	51°15′53·679″	1·26	0·58	Gastropod	1370 ± 130
C4-1	Core 4	26°8′40·0524″	51°16′25·683″	1·62	1·75	Gastropod	6060 ± 150
C4-2	Core 4	26°8′40·0524″	51°16′25·683″	1·62	1·6	Gastropod	6730 ± 160
C4-3	Core 4	26°8′40·0524″	51°16′25·683″	1·62	0·8	Gastropod	5750 ± 140
C4-4	Core 4	26°8′40·0524″	51°16′25·683″	1·62	0·78	Gastropod	5980 ± 170
C5-1	Core 5	26°9′30·762″	51°16′30·2658″	0·98	3·82	Coral*	3900 ± 170
C5-2	Core 5	26°9′30·762″	51°16′30·2658″	0·98	3·58	Coral*	3660 ± 160
C5-3	Core 5	26°9′30·762″	51°16′30·2658″	0·98	3·45	Bivalve	1450 ± 140
C5-4	Core 5	26°9′30·762″	51°16′30·2658″	0·98	1·75	Worm tube	1380 ± 120
C5-5	Core 5	26°9′30·762″	51°16′30·2658″	0·98	0·85	Bivalve	810 ± 130
C5-6	Core 5	26°9′30·762″	51°16′30·2658″	0·98	0·05	Gastropod	980 ± 120
C6-1	Core 6	26°9′33·6528″	51°16′25·5498″	0·58	3·1	Gastropod	2270 ± 160
C6-2	Core 6	26°9′33·6528″	51°16′25·5498″	0·58	2·96	Gastropod	2610 ± 160
C6-3	Core 6	26°9′33·6528″	51°16′25·5498″	0·58	2·96	Gastropod	1900 ± 160
C6-4	Core 6	26°9′33·6528″	51°16′25·5498″	0·58	2·24	Gastropod	1130 ± 140
C6-5	Core 6	26°9′33·6528″	51°16′25·5498″	0·58	1·2	Gastropod	1100 ± 140
C6-6	Core 6	26°9′33·6528″	51°16′25·5498″	0·58	0·8	Gastropod	1030 ± 140
C7-1	Core 7	26°9′20·073″	51°16′15·6288″	0·84	2·55	Coral	2080 ± 180
C7-2	Core 7	26°9′20·073″	51°16′15·6288″	0·84	1·95	Coral	2060 ± 180
C7-3	Core 7	26°9′20·073″	51°16′15·6288″	0·84	1·75	Gastropod	1040 ± 130
C7-4	Core 7	26°9′20·073″	51°16′15·6288″	0·84	0·65	Gastropod	130 ± 130
C7-5	Core 7	26°9′20·073″	51°16′15·6288″	0·84	0·15	Gastropod	120 ± 120

NA, not available.
* InPlace.

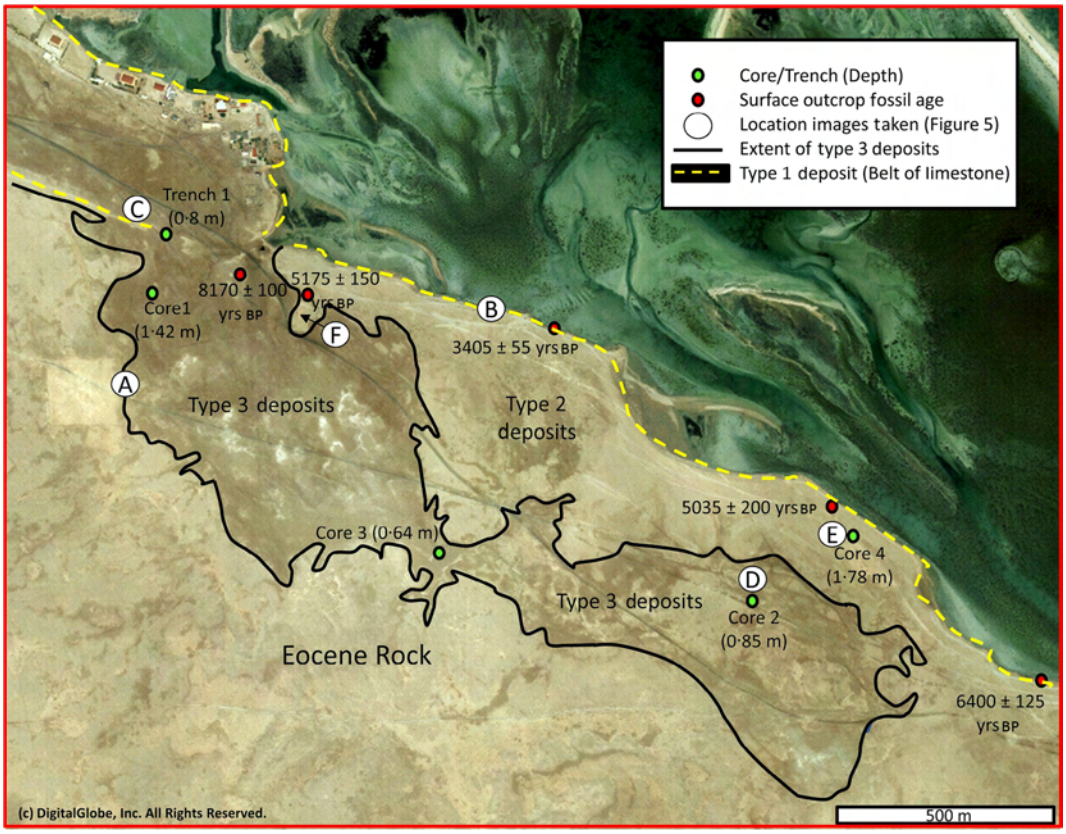

Fig. 4. WorldView-2 (2015) image of the onshore Al Ruwais area showing the location of various types of deposits as well as trench and vibracore locations and penetration depths, photograph locations for Fig. 5 and ^{14}C dates from surface fossils. See text and Table 2 for more information on deposit types.

ONSHORE SURFACE OBSERVATIONS

The ^{14}C ages of molluscs taken from surface exposures show that mid-Holocene age deposits can be found along the landward shoreline of the modern lagoon in the Al Ruwais region, extending landward *ca* 600 m before onlapping the underlying Eocene bedrock (Table 1; Figs 3, 4 and 5A). Onshore deposits can be broadly segregated into three types based on surface observations (Table 2).

Continuous linear limestone rock outcrops forming type 1 deposits (Fig. 4) may be observed: (i) to the south-east along the landward shoreline of the modern restricted intertidal (lagoon) system having overlying carbonate sands (Fig. 5B); and (ii) extending north-westward both alongshore and onshore, where

Fig. 5. Field photographs, locations of (A) to (F) shown in Fig. 4. (A) Image looking south-east at the contact between Holocene sediment and Eocene bedrock. For scale, shrubs in the foreground range from 1 to 5 dm in width. (B) Image looking eastward to lithified mid-Holocene deposits representing the seaward margin of the type 1 deposits exposed along the inner edge of the modern lagoon. Seaward-dipping planar bedding indicates palaeobeach deposits. Field vehicle for scale 1·8 m high. (C) Break in outcrop of lithified mid-Holocene type 1 deposits, interpreted as a tidal inlet, where trench 1 was excavated. Field vehicles for scale. (D) Image looking north (seaward) from a low-lying area occupied by type 3 mid-Holocene deposits to type 2 deposits behind. Mangroves on the horizon mark the location of the type 1 deposits that lie along the landward shoreline of the modern lagoon. Note tyre tracks in the foreground (25 cm wide) for scale. (E) Surface exposure of stromatolites (type 2 deposits) landward of type 1 deposits. Field vehicle for scale. (F) Image showing vertical trace fossil tubes common to type 2 deposits. Bottle for scale, 20 cm wide. (G) Crab burrows, similar to trace fossils shown in Fig. 4F, but located in the modern intertidal zone behind Umm Tays Island (lithified example) and in the modern intertidal along the Gulf of Salwa coast (unlithified example inset). Foot and finger for scale. (H) Image showing lithified relict (late Holocene) linear deposit of carbonate grainstone sitting directly upon moribund reef. Person for scale is *ca* 1·8 m tall.

overlying sands are not observed (Fig. 5C). In all instances type 1 deposits have typical elevations of >1·3 m above mean sea-level (msl). The lithified deposits are grainstones that contain large clasts (up to tens of centimetres) of dolomitized Eocene bedrock, as well as whole mollusc shells and fragments thereof. Other allochems identified in these rocks include red algal fragments, coral fragments, coated grains, benthic foraminifera (rotalids and miliolids) and intraclasts (Fig. 6). Low-angle (<5°) inclined bedding has been recognized in these deposits, and bedding commonly dips seaward (Fig. 5B). Cements are typically of two types, bladed Mg-calcite and cryptocrystalline Mg-calcite, and their order of precipitation varies (Fig. 6A and B). The cryptocrystalline cements commonly show a meniscus fabric (Fig. 6A), and so are not interpreted as depositional mud. Clotted textures have been observed in these rocks (Fig. 6B). Allochems observed in the overlying unlithified carbonate sands (observed in the south-east) are similar to those of the underlying grainstones.

Variably-lithified type 2 sediments lie directly landward of type 1 deposits, extending 100 to 500 m southward, with a lobate landward margin (Fig. 4). These deposits occupy slightly lower elevations relative to type 1 deposits, commonly 1·0 to 1·3 m above msl (Fig. 5D) and include lithified features (Fig. 5E) identical in shape to modern microbial mats of Al Ruwais (Fig. 2; upper left insert), although the possibility that the features represent mud cracks cannot be completely discounted. Limestones with innumerable vertical tubes are also commonly found in this area (Fig. 5F), as are both lithified and unlithified *cerithid* gastropod deposits. Further landward, low-lying (<1 m above msl) unlithified type 3 deposits include carbonate mud and sand with similar allochems to those found in type 1 and 2 deposits. Type 3 deposits variably extend between 100 m and 500 m southward of type 2 sediments, and onlap Eocene bedrock.

Four vibracores (cores 1 to 4) were taken and one trench (trench 1) was excavated in the onshore Al Ruwais area, all of which reached the underlying Eocene bedrock <2 m beneath the surface (Figs 4 and 7). Allochems in cored sediments are similar to those observed at the surface, and include significant quantities of molluscs, red algae and Eocene rock fragments. The cored sediment from deposit type 2 is mostly carbonate sand, whereas sediment from deposit type 3 is mostly of wackestone or packstone texture (Fig. 7).

UMM TAYS ISLAND SEDIMENTS AND VIBRACORE DESCRIPTIONS

The nature of recent sedimentary deposits in the area of Umm Tays Island has been reviewed in detail by Purkis *et al.* (2017). Surface sediments

Table 2. Onshore deposit types at Al Ruwais.

Deposit type	Distribution	Elevation above msl	Allochems	Textures	Observations
1	Linear Belts	1·3 to 1·6	Eocene bedrock clasts, mollusc shells, red algal fragments, coral fragments, coated grains, benthic foraminifera and intraclasts	Grainstone	Rocks with gently seaward-dipping bedding overlain locally by carbonate sands. Rocks are cemented by bladed and crypocrystalline Mg-calcite cements with common meniscus fabrics
2	Lobes	1·0 to 1·3	As type 1 with higher concentrations of gastropods	Grainstone and minor packstone	Lithified microbial mats or mudcracks, variably lithified gastropod-dominated deposits, crab burrows
3	Irregular Lenses	0·7 to 0·9	As type 1	Packstone and wackestone	Unlithified mud-bearing deposits with pedogenic overprint

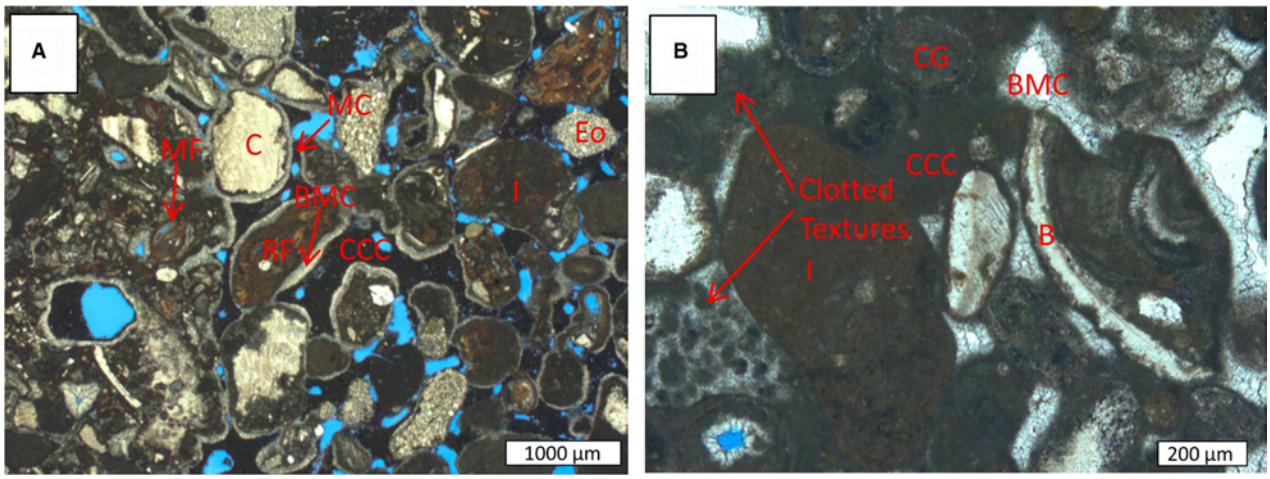

Fig. 6. Thin section microphotographs. (A) Image of rock from of type 1 deposit showing common allochems and cements. Meniscus cements (MC) are common. (B) Image of rock from type 1 deposit showing allochems, cements and clotted textures. B, bivalve; BMC, bladed Mg-calcite cement; C, coral; CCC, cryptocrystalline Mg-calcite cement; CG, coated grain; Eo, Eocene clasts (recrystallized dolomite); I, intraclast; MF, miliolid foraminifera; RF, rotalid foraminifera.

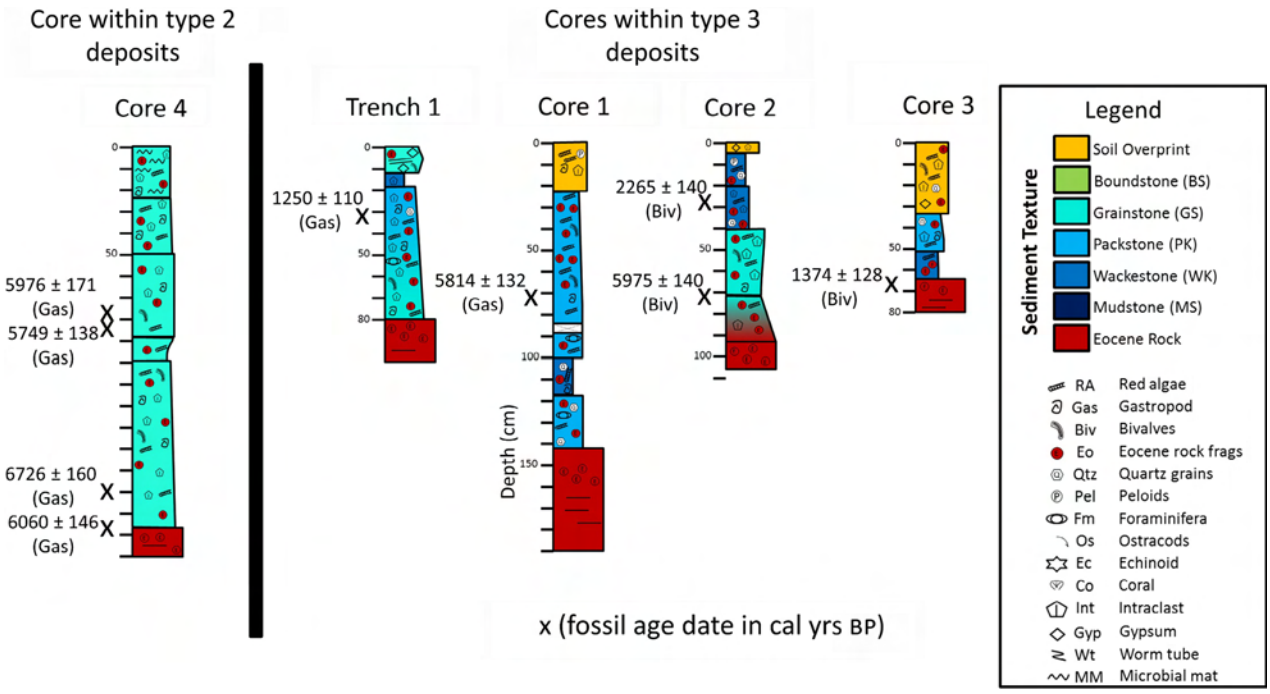

Fig. 7. Descriptions and fossil dates for onshore cores delineated by deposit type. Core and trench locations are shown in Fig. 4.

generally lack mud. The upper shoreface of the open coast, as well as the seaward-facing barrier beach and associated aeolian dunes, are characterized by the presence of coarse to very coarse coralgal sands. The intertidal to subtidal lagoon landward of the barrier island displays more variable, but generally finer grain-size distribution, ranging from fine to very coarse sand. Common back-barrier allochems include peloids, as well as coral, and red algal remains. To augment these observations, three vibracores (cores 5, 6 and 7) were taken on Umm Tays Island (Fig. 8A). Core 5 was taken on the modern barrier beach, where muddy sediment was

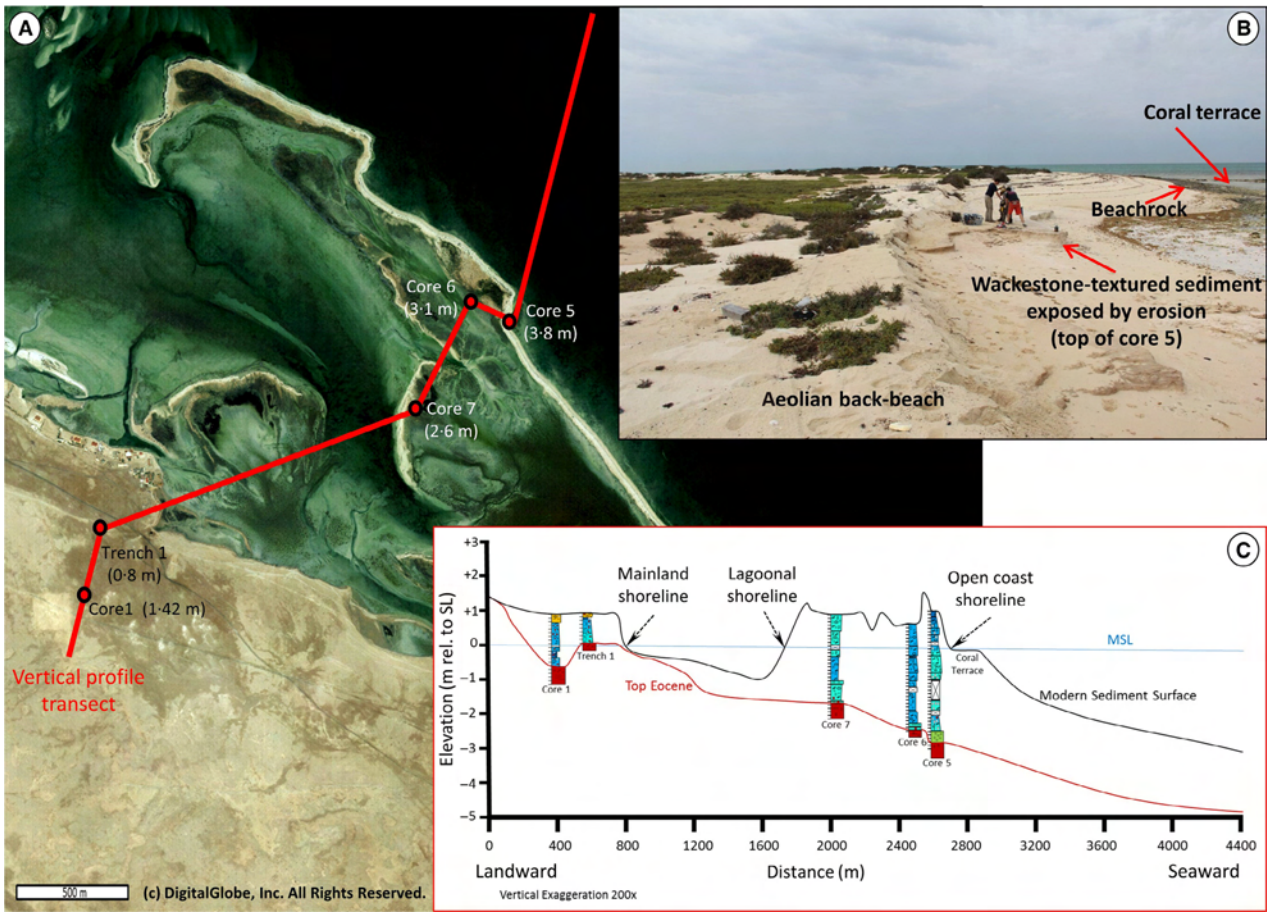

Fig. 8. (A) Satellite image (WorldView-2, 2015) showing location of cores 5 to 7 relative to core 1 and trench 1. The red line shows the location of the cross-section shown on the bottom right. (B) Image of core 5 being extracted from eroding muddy layer on the seaward side of Umm Tays Island. People for scale are *ca* 1·8 m tall. (C) Cross-section – see (A) for location – showing cores positioned at their measured elevations. The topography of the modern surface and the top the Eocene are estimated between the core and trench control points.

exposed by erosion in the beach swash zone during high tide (Fig. 8B). Cores 6 and 7 were recovered from the modern intertidal back-barrier area. Figure 8C is a cross-section representing the transect line shown in Fig. 8A, with cores hung at their measured elevations.

Holocene deposits on Umm Tays Island are thicker than onshore equivalents, ranging between 2·6 m and 3·8 m of sediment (Fig. 9). Coral boundstone (*Platygyra*) is observed at the base of core 5 and coral-rich sands containing large coral fragments are observed at the base of cores 6 and 7 (Fig. 9). The coral-rich sediment is underlain in core 6 by a thin but conspicuous well-cemented grainstone (Fig. 9), with cement morphologies identical to those observed in onshore type 1 deposits (Fig. 6). Lying directly above the coral deposits are grainstone and packstone-textured sediments rich in fragments of red algae, corals, peloids and mollusc shells. The carbonate mud content observed in the cores is higher than that found by the Purkis *et al.* (2017) study of surface deposits.

DEPOSITIONAL INTERPRETATIONS AND EVOLUTIONARY MODEL

Onshore, type 1 deposits contain allochems including clasts from the underlying Eocene rocks, as well as detrital skeletal grains and fragments from the Holocene carbonate depositional system ^{14}C-dated to have formed between 8270 and 3350 cal yr BP (Table 1; Fig. 4). Remembering that these dates represent when individual shells formed, not when they reached their final depositional position, type 1 rocks and sediments were deposited, at least in some part, after 3350 cal yr

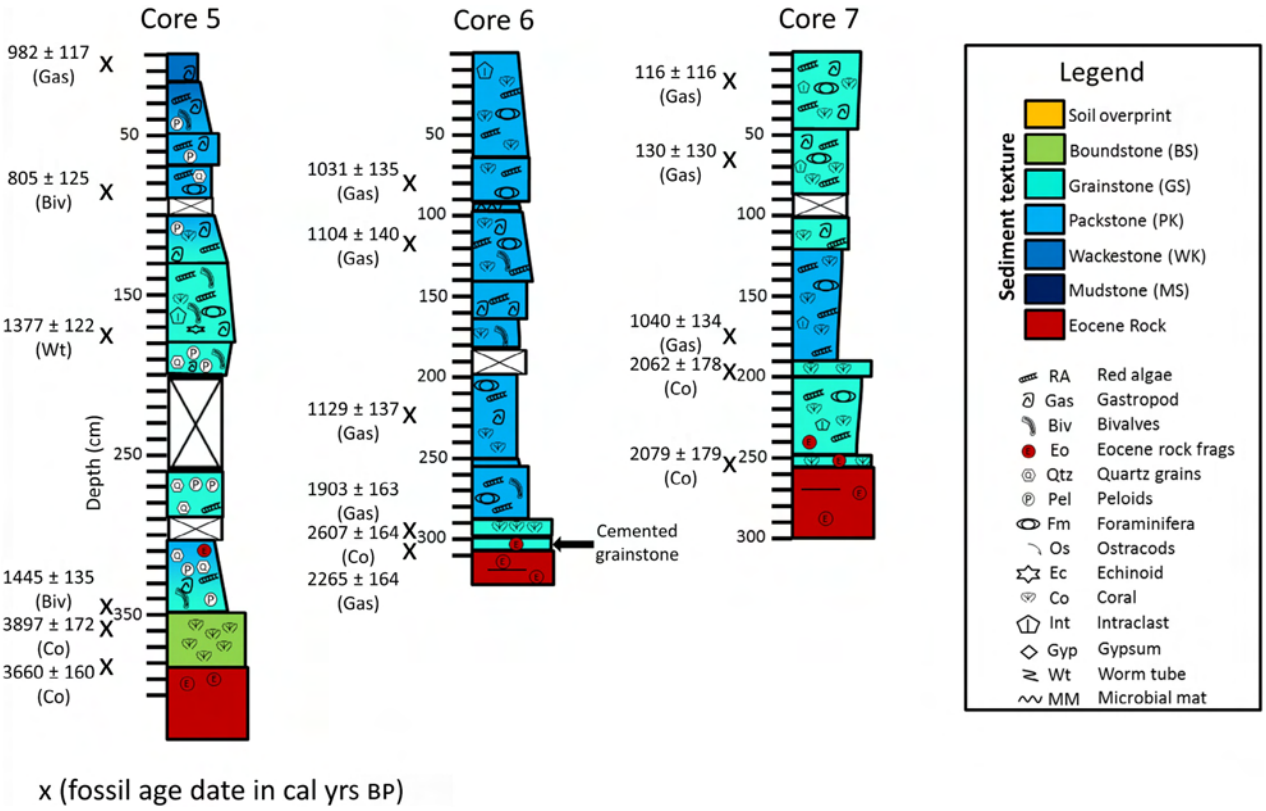

Fig. 9. Descriptions of cores from Umm Tays Island with associated fossil dates.

BP (Fig. 3). The rocks are cemented by both bladed and cryptocrystalline high Mg-calcite cements (Fig. 6A and B), both of which commonly form in marine waters (e.g. James & Choquette, 1990a; Scholle & Ulmer-Scholle, 2003) or mixed marine–meteoric waters (Mauz *et al.*, 2015), whereas the meniscus-like fabric of the cements indicates that they formed partly in vadose settings (James & Choquette, 1990b) overlying marine waters. Clotted, or micropeloidal cement textures (Fig. 6B) are indicative of microbial activity (Scholle & Ulmer-Scholle, 2003), evidence of which has been previously observed in association with beachrock cement (Webb *et al.*, 1999). The linear shape of grainstone bodies, texture and age dates, as well as cement mineralogy and fabric, all point to lithified type 1 deposits as being mid-Holocene beachrock deposits (cf. Vousdoukas *et al.*, 2007). The allochem content of these rocks, rich in molluscs, coral fragments and red algal remains, shows that the depositional system during this time was similar to that of today, and incorporation of Eocene clasts reflects the presence of the underlying bedrock exposure surface over which the sea transgressed. The elongate, coast-parallel geometry of the type 1 deposits supports a foreshore interpretation. Almost identical deposits (with fewer Eocene grains) are found today along the seaward-facing beaches of Umm Tays and Jazeerat Reken barrier islands (Fig. 8B). The overlying unlithified carbonate sands found in association (Fig. 5B) are interpreted as the remnants of back-beach aeolian dune deposits, equivalent to those observed along the modern island beach systems (Fig. 8B).

Surface features of type 2 rocks include lithified remains of microbial mats (stromatolites) or possibly mud cracks (Figs 5E and 7; core 4), with features identical to microbial mats found in the modern back-barrier of Jazeerat Reken island (Fig. 1). Other rocks display tubular features (Fig. 5F) identical to those in rocks and sediments from the modern back-barrier intertidal settings (Fig. 5G), that are interpreted to have formed through the burrowing action of crabs, very commonly observed in the modern depositional system (Fig. 2). Considering their location relative to the beach deposits (type 1) as well as their depositional features, and the prevalence of *cerithid* gastropods, type 2 deposits are most likely back-beach intertidal sediments and rocks that formed landward of a mid-Holocene beach (Fig. 10). In

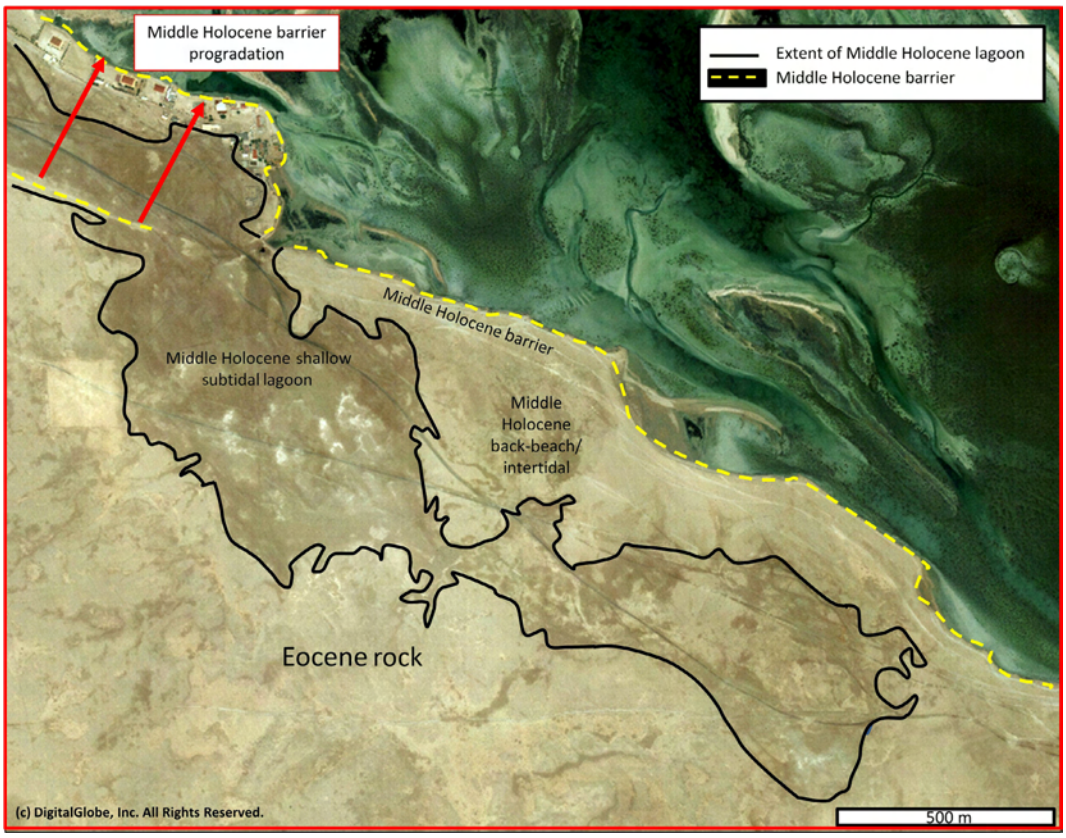

Fig. 10. Same area as in Fig. 4 but showing interpreted depositional environments, and inferred barrier progradation during the middle Holocene.

the modern system, the elevation of the land surface decreases from the carbonate aeolian deposits (McKee & Ward, 1983) to landward intertidal settings, where microbial mats and crab-burrowed sand flats in various stages of lithification are common (Fig. 3). Concentrated *cerithid* deposits can be found along the margins of microbial mats upon which they graze. The lobate geometry of the landward margin of these type 2 deposits (Fig. 4) suggests the presence of washover lobes/fans and/or lobate flood-tidal deltas.

Satellite imagery of type 3 deposits shows that they are commonly darker in colour relative to type 2 equivalents, likely reflecting greater water retention in these finer sediments (Figs 4 and 5D). Cores 1, 2 and 3 were taken from type 3 deposits, within which trench 1 was also excavated (Fig. 7). Supporting surface observations, the cores demonstrate that type 3 sediments are mostly of packstone and wackestone texture. The allochems in these cores are similar to those found in both the mid-Holocene beachrocks and generally throughout the modern depositional system. The ^{14}C-dating of both surface and shallow subsurface fossils show these deposits to have formed mostly prior to 1400 years ago (Table 1). Based on their distribution, low elevation, higher mud content, allochem content and age, type 3 deposits are interpreted as mid-Holocene lower energy, subtidal lagoonal sediments (Fig. 10). The presence of these sediments indicates that type 1 foreshore deposits were not land-attached, but that they represent a mid-Holocene beach barrier protecting a back-barrier lagoon. Breaks in type 1 deposits are interpreted to represent inlets, connections between the open gulf and the back-barrier lagoon (Fig. 5C). Such openings are smaller than the tidal inlets in the modern barrier (Fig. 2) likely because of the smaller surface area of the mid-Holocene lagoon, and the resulting smaller tidal prism (cf. Dalrymple, 2010). Trench 1 (Fig. 7) shows that sediments deposited in these inlets were grainy with muddy sediments only occurring at the top of the trench, likely representing abandonment of the mid-Holocene barrier system.

Deposits recovered from vibracoring on Umm Tays Island (Fig. 9) indicate that environments

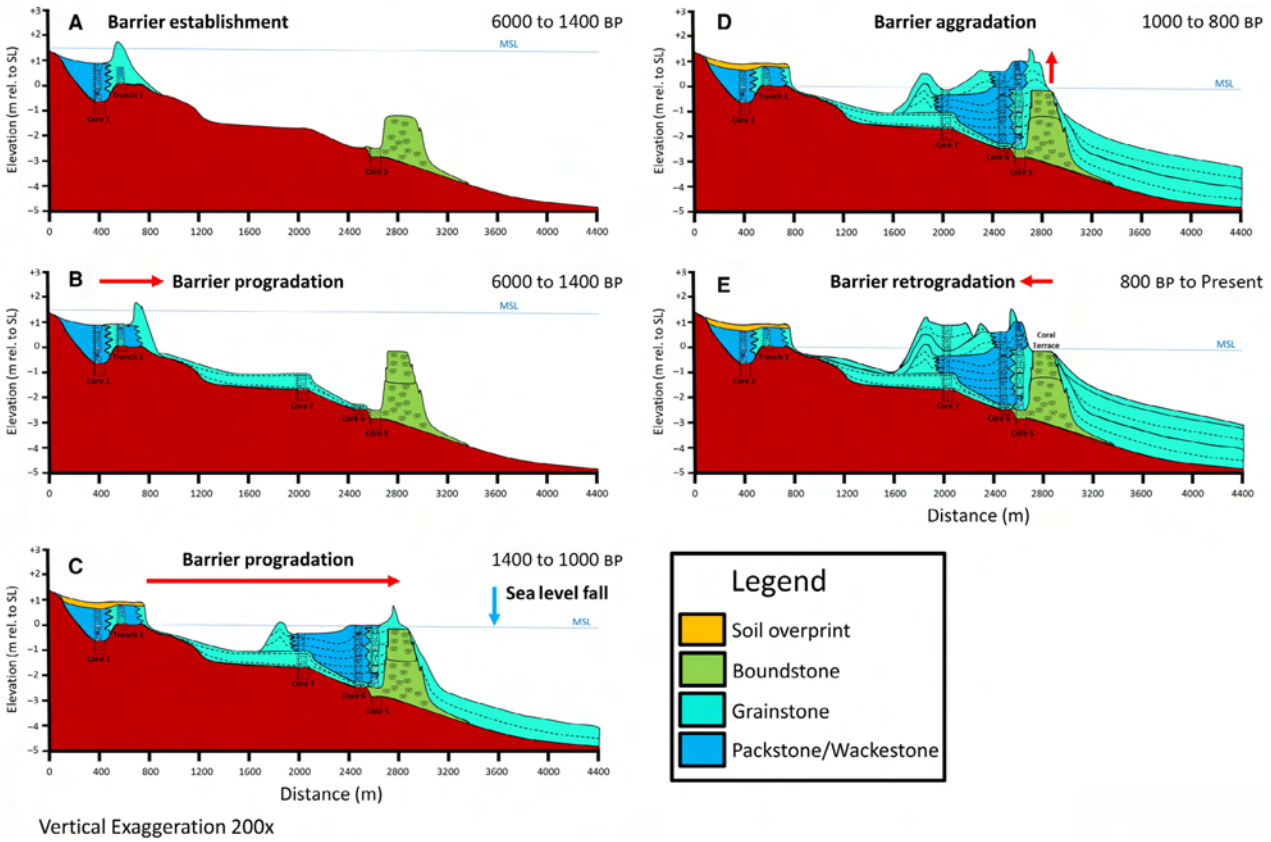

Fig. 11. Model showing interpreted evolution of the Al Ruwais carbonate depositional system during the Holocene: (A) and (B) Mid-Holocene (7000 to 1400 BP); (C) Late Holocene (1400 to 1000 BP); (D) Late Holocene (1000 to 800 BP); and (E) recent deposition (800 BP to present). Colours in the model correspond to texture colours in core descriptions (see Figs 7 and 9).

of deposition have evolved there during the late Holocene. Immediately above the Eocene contact, in-place coral boundstone or coarse coral-rich sands were observed in cores 5 and 7. At the core 6 location, a thin layer of grainstone with beachrock-type cements separates similar coral deposits from the Eocene rock (Fig. 9). The corals from these cores were dated to have formed between *ca* 3900 and 1900 years ago, whereas somewhat younger ages (1460 to 1510 years ago) were obtained from samples of the coral terrace exposed immediately seaward of Umm Tays Island (Table 1; Fig. 8B). In all Umm Tays Island cores, the coral deposits are immediately overlain by both muddy and grainy sediments rich in molluscs and red algae. These deposits formed after *ca* 1400 years ago, and are similar to, but muddier than, those currently being deposited in the modern back-barrier area (Purkis *et al.*, 2017). Due to their allochem and mud content, these sediments are interpreted to represent recent back-barrier deposits. Linear belts of lithified grainstones sitting directly on the moribund reef systems (Fig. 5H) up to 200 m seaward of the modern barrier likely represent older beachrock deposits, similar to those found fronting the modern beach (Fig. 8B), indicating the previous (although recent) position of the barrier beach. The exposure of mud-supported back-barrier deposits by erosion in the modern foreshore (Fig. 8B) also attests to the landward migration of this barrier.

To summarize, the evidence presented above points to a barrier/back-barrier-lagoonal system having migrated significant distances in both seaward and landward directions since the mid-Holocene. The exact timing of these changes is complicated by the fact that ^{14}C dating determines when a shell was formed, but not when a deposit incorporating the shell was formed. Therefore, ages of detrital grains should be assumed to be older than the deposit itself to some degree. Also, although care was taken in selecting pristine, cement-free shell for dating, carbon from fossil

shells can be contaminated by more recent diagenetic products, skewing the dates to younger ages. In spite of these limitations, the ^{14}C dates obtained for detrital grains during this study can be used with a regional understanding of the sea-level history (Fig. 3), as well as age dating of in-place coral samples and the law of superposition to broadly reconstruct the timing of events.

Based on regional studies (Lambeck, 1996), prior to 7 ka the Al Ruwais region was exposed to the meteoric environment as the ocean had not yet risen to the modern level (Fig. 3). Between 7 ka and 5 ka the area was flooded by marine waters and sea-level rose to *ca* 1·6 m higher than the current level, based on the elevation of the lithified stromatolites or mud cracks (both assumed to be intertidal) at the core 4 location (Fig. 5E). This elevation is in agreement with the elevations of onshore beachrock occurrences, 1·3 to 1·6 m (Table 1), which are considered to be useful as indicators of previous sea-level (Kelletat, 2006; Desruelles *et al.*, 2009; Mauz *et al.*, 2015). During this time a beach-barrier was established along the location of the modern mainland shoreline (Fig. 10) with tidal openings and a narrow back-barrier intertidal-flat and lagoon system behind it (Fig. 11A). Stepwise progradation of the barrier system occurred in the north-western portion of the onshore study area as shown by the presence of two ridges of type 1 deposits (Figs 10 and 11B), whereas no evidence of similar progradation is found to the south-east. Seaward of the barrier, an extensive shore-parallel coral reef flourished contemporaneously, based on dates of in-place corals, at the position of, or immediately fronting the modern barrier islands (Fig. 8B). The narrow barrier/coral system persisted until *ca* 1400 years ago based on the youngest onshore fossil dates (Table 1), with one onshore date from trench 1 (1250 $\pm$ 110 years) giving a slightly younger date.

As sea-level dropped to near current levels *ca* 1400 years ago (Fig. 11C), a major rearrangement of the Al Ruwais depositional system occurred in which the landward barrier system was exposed, and the coral reef met its demise. The interpreted timing and magnitude of the sea-level fall is in good agreement with that determined by Lokier *et al.* (2015) for elsewhere in the Arabian Gulf. Based on the observation that linear beachrock deposits cap parts of the coral reef seaward of the modern barrier island, a new barrier system was apparently established directly on top of the coral reef (Figs 5H and 8B), most likely in response to the establishment of significant wave-energy dissipation on the reef as water depth decreased during the sea-level fall. Assuming that detrital grains give some estimate, back-barrier sediments penetrated by cores 5, 6 and 7 on Umm Tays Island accumulated between *ca* 1400 to 800 years ago (Fig. 11C and D). Since that time the barrier has both aggraded (at core 7 position) and retreated *ca* 200 m landward based on the separation between the fossil beachrock on the reef crest and the immediately adjacent modern beach (Fig. 5H). This back-stepping is confirmed by the observation that back-barrier sediments are exposed in the modern shoreface by ongoing erosion at core position 5 (Figs 8B and 11E). Modern barrier retreat likely created the northwesterly tombolo-like attachment to Jazeerat Reken Island (Fig. 2), indicating that the barrier there has retreated as much as 1 km since its inception.

DISCUSSION

The origin of barrier islands at Al Ruwais

Three modes of barrier island formation have been postulated (Davis, 1994): (i) vertical aggradation and exposure of sub-aqueous sand bars (De Beaumont, 1845); (ii) lateral accretion of land-attached sand spits, later dissected and separated from land by breaches caused by tide-related and wave-related erosion (Gilbert, 1885); and (iii) coastal submergence causing isolation of coastal ridges (McGee, 1890). Lateral accretion of land-attached spits, and resulting formation of carbonate cheniers (Billeaud *et al.*, 2014) and mixed carbonate–siliciclastic strand plains (Strohmenger & Jameson, 2015) is a common depositional motif along the Qatar coastlines. At Al Dakhirah, 50 km south-east of Al Ruwais (Fig. 1), successive seaward formation of laterally-accreting carbonate spits and infilling of landward lagoons has been associated with 3 km of shoreline progradation forced by the late Holocene regression (Billeaud *et al.*, 2014). Aerial photography of the Al Ruwais region from 1963 shows the system prior to coastal building construction (Fig. 12). The image demonstrates two successive phases of spit formation (S1 and S2) nucleated from Eocene bedrock highs in the mid-Holocene based both on S1 sediment age dates in this study, and the similar elevation (+1·5 m) of S1 and S2, in agreement with the regional Holocene sea-level

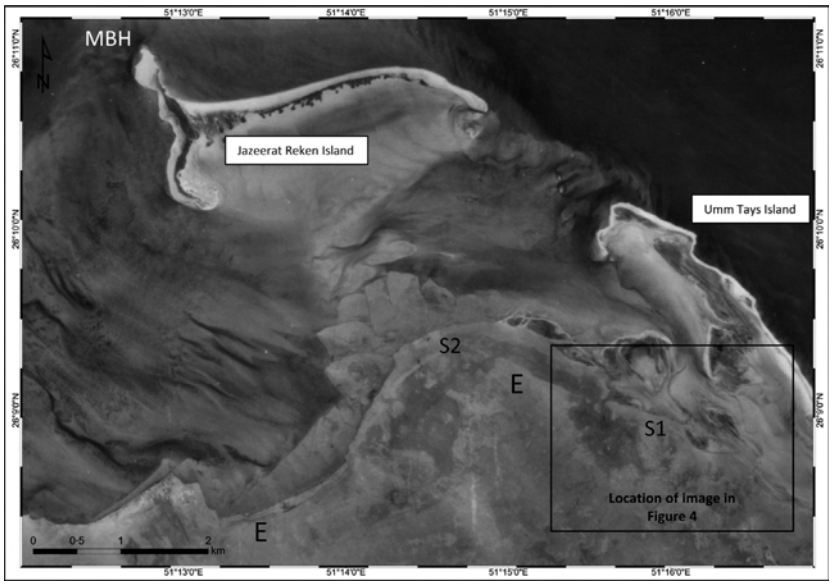

Fig. 12. A 1963 aerial photograph of the Al Ruwais region prior to coastal building construction. Land-attached (i.e. Eocene-bedrock-attached) spits are apparent onshore (S1, S2). Eocene bedrock labelled 'E'. A modern barrier headland (MBH) is attached to Jazeerat Reken Island and is interpreted as a remnant of an earlier island, that may have been one source of sediment for the modern barriers. Photograph courtesy of the Qatar Ministry of Municipality and Environment.

curve (Fig. 2). Lateral accretion of the spits appears to have occurred from the north-west to the south-east, in alignment with the present wind and wave directions (Yousif *et al.*, 2018). Lateral accretion of spit system 2, observed to cause stepwise progradation in the north-western portion of the mid-Holocene system (Fig. 10), perhaps did not continue to the south-east because it was abandoned during sea-level fall. It is also possible that the south-western portion of S2 retreated and amalgamated with S1 prior to sea-level fall.

The mode of formation of the late Holocene barrier island is more uncertain. Because the modern barrier islands formed directly on a mid-Holocene carbonate reef during sea-level fall, coastal submergence causing isolation of coastal ridges can be dismissed as a possibility for late Holocene barrier island formation at Al Ruwais. Spit-like lateral accretion is undoubtedly important in the formation of the modern barrier, because recurved-spit morphology is clearly visible in some areas. Images of the system, however, do not indicate that the barrier was ever land-attached, as observed of the mid-Holocene deposits (Fig. 12). Jazeerat Reken Island is attached to a modern barrier headland (Fig. 12). This island may have formed through localized exposure of a portion of the mid-Holocene reef, although no visual evidence is observed of any part of the reef having been exposed there or elsewhere in the system. Alternatively, and perhaps more likely based on the observed linear beachrock deposits overlying the reef elsewhere (Fig. 5H), upon sea-level fall, and the seaward migration of the intertidal zone to the reef crest, the modern barrier island formed as the result of loose sediment deposition upon the reef top by wave action followed by upward accretion and emergence. In either case, the headland appears to be too small to have supplied all of the sediment comprising the modern barrier chain. This study interprets that the late-Holocene shallowing of the mid-Holocene shore-parallel reef caused nucleation of an overlying beach-barrier, with much of the sediment forming the barrier being cannibalized from the reefal material found seaward, and in the updrift 'headland'.

Carbonate barrier islands systems: an underappreciated depositional model?

The setting in which the mid-Holocene and modern barrier-island systems at Al Ruwais exist falls within the general parameters understood to be necessary for the formation of siliciclastic barrier islands (Davies, 1964; Hayes, 1979; Davis *et al.*, 2004), in that it is a low-gradient, micro-tidal coastal area with wave heights of <2 m. The necessary sediment supply (Davis, 1994) would appear to be predominantly from nearby shallow-subtidal areas based on the composition of the grains (Purkis *et al.*, 2017). The observed decrease in average grain size from the barrier to the lagoon is also seen in siliciclastic systems (Davis, 1994). Aside from the beach barriers themselves, common geomorphic components of siliciclastic barrier systems (Flemming, 2012) are also found in the Al Ruwais system (Fig. 2) including aeolian dunes, tidal inlets and

back-barrier channels, flood-tide and ebb-tide deltas, and washover fans, as well as back-barrier microbial mats, tidal flats and mangrove forests in place of salt marshes. Erosion and migration of tidal inlets is indicated by the curvature of the bracketing barrier deposits (i.e. recurved spit morphology; Fig. 12), processes observed in siliciclastic systems (Hayes, 1979). Therefore, in terms of depositional setting, general grain-size trend, geomorphology and depositional processes, the carbonate barrier island system at Al Ruwais is identical to those of the siliciclastic realm. This is similarly true for the setting, grain-size trend and geomorphic components of the barrier island system fronting the Terminos Lagoon in the Gulf of Mexico (Phleger & Ayala-Castanares, 1971). Given the observations above it is clear that, provided the oceanographic and geomorphic settings are similar, siliciclastic-style barrier island systems can occur in the carbonate realm, apparently through similar processes of formation.

Several questions arise from this basic observation. First, can carbonate barrier-island systems form on an open shelf or ramp, and migrate long distances landward during transgressions as siliciclastic islands do, or do they mostly form on palaeo-topographic highs, being anchored in place by early marine and meteoric cementation? Second, why are carbonate barrier island systems not more common along modern coasts of the carbonate realm? Third, were carbonate barrier island systems likely more common in the geological past?

Assuming that the above interpretations are correct, this study of barrier island formation at Al Ruwais demonstrates that carbonate barrier islands can form both from dissection of land-attached spits (mid-Holocene example) and nucleation on pre-existing ridges (late Holocene example). Although the Al Ruwais example demonstrates that barrier islands can form in the same way that their siliciclastic counterparts can, it is plausible that landward migration of carbonate barrier islands, especially of aragonite-rich deposits in humid settings, might be inhibited relative to siliciclastic counterparts as a result of early marine and meteoric cementation. In the arid aragonite-rich system of Al-Ruwais, however, such migration is documented for both barrier systems, despite cementation (i.e. beachrock formation) of the foreshore. Landward migration is indicated for the mid-Holocene spit-related barrier system by the presence of beachrock deposits that underlie the mid-Holocene coral deposits in core 6 (Fig. 9), which proves that the mid-Holocene beach formed kilometres seaward of (and presumably before) the onshore mid-Holocene barrier beach deposit. Landward migration is proven for the late Holocene barrier, both by the existence of beachrocks marking previous barrier locations (Fig. 5H) as much as 200 m seaward of the current barrier beach, and by the exposure of fine back-barrier sediments on the modern barrier beach through erosion of the foreshore (Fig. 8B). Assuming that the modern barrier headland to the north-west (Fig. 12) marks the initial nucleation point of Jazeerat Reken Island, *ca* 1 km of landward migration of that barrier likely occurred since its initial formation, in the process forming a tombolo that extends south-eastward from the rocky island. Recent landward migration may be occurring in association with sea-level rise (Alothman *et al.*, 2014). The mobility of meteorically-exposed, aragonite-rich carbonate sand bodies in an arid setting can also be observed south-eastward of Al Ruwais at Al Dakhirah. Here carbonate spits are constantly forming and reforming over decadal time periods (Billeaud *et al.*, 2014). In the more humid southern Gulf of Mexico, the possibility of landward migration of the carbonate barrier islands fronting the Terminos Lagoon cannot be assessed; however, significant modern shoreface erosion is documented (Phleger & Ayala-Castanares, 1971). Indeed, Google Earth® images show traces of a recurved-spit morphology in shallow water to the north of the lagoon. Based on these shapes, up to 1 km of landward migration of the carbonate beach is implied. Therefore, the presence of beachrock cementation is apparently not a major impediment to the migration of carbonate barrier islands.

The relative scarcity of carbonate barriers in modern warm-water coastal depositional systems remains an issue demanding explanation. With regard to the Qatar coastlines south of Al Ruwais, land-attached beaches are observed. In some areas kilometres of strand plain (Strohmenger & Jameson, 2015) and chenier (Billeaud *et al.*, 2014) progradation has occurred over the past 6000 years in conjunction with the recent regression. Such depositional motifs are more common along regressive wave-dominated shorelines (Plint, 2010). Since most mobile-type barrier islands form on transgressive coastlines, formation of barrier islands at Al Ruwais during the recent regression is unusual, and likely results from the emergence of the fringing reef

that formed immediately prior to sea-level fall, allowing nucleation of a barrier while retaining accommodation for back-barrier subtidal settings.

More broadly, several possibilities may explain why carbonate barrier islands are less common than siliciclastic equivalents. The nature of shallow water flat-topped carbonate platforms greatly limits the amount of wave energy reaching inner-platform shorelines. This reflects damping of open-ocean waves at platform margins by the presence of shallow subtidal reefs and grain shoals, as well as emergent equivalents of the same that form islands. As a result tidal flats can be developed instead of beaches along inner platform highs (cf. the western coast of Andros Island, the Bahamas). The platform-marginal grainy systems are not observed to migrate platformward significantly for several reasons. First, coral reefs form large, hard, relatively immobile structures that can keep up with sea-level rise (Davis, 1985; James & Macintyre, 1985; Neumann & Macintyre, 1985), second, early marine and meteoric (in the case of islands) cementation is common (James & Choquette, 1990a,b) and third, on large platforms, such as the Bahamas, grain belts generated in these settings are commonly wide (>5 km) (Harris *et al.*, 2011). The width of these belts reflects the presence of a line-source of sediment (skeletal and non-skeletal grains forming at the margin) that is redistributed platformward by tidal energy. Tidal-current action is amplified at the margin of continental shelves and platforms (Fleming & Revelle, 1955; Reynaud & Dalrymple, 2012). These margin-linked tidal shoals will be less prone to migration than a thin wave-formed barrier island system of any composition.

On open shelves, the direction of sediment supply may increase the propensity for siliciclastic barrier islands to form relative to detrital carbonate equivalents. In siliciclastic settings, the sediment source is typically an eroding headland composed of unconsolidated sediment, with the sediment moving alongshore in the shallow water nearshore zone of high wave energy. As a result, sediment availability is generally not a significant limitation. On open carbonate shelves, by contrast, eroding headlands are not common; instead, the sediment must be moved onshore from the shoreface and/or inner shelf, a source that is indicated by the ecology of the organisms comprising the barrier superstructure (e.g. Joury *et al.*, 2018). This onshore movement of sediment, especially if the sediment comes from the lower shoreface and inner shelf, is much less efficient than alongshore movement because normal fair-weather wave action is thought to move sediment onshore from relatively shallow depths (i.e. the upper shoreface; Niedoroda *et al.*, 1984; Storms, 2003; Aagaard *et al.*, 2004; Joury *et al.*, 2018). Onshore movement from greater depths requires larger, non-storm waves, because large storm waves typically lead to erosion and net seaward transport of sediment seaward (Niedoroda *et al.*, 1984; Storms, 2003; Brill *et al.*, 2016). Significant nourishment of barriers in carbonate settings may therefore be dependent on the action of swell waves (cf. Backstrom *et al.*, 2009). This process, however, appears not to supply sediment as rapidly as longshore transport, so the formation of a carbonate barrier might be limited by sediment availability. Further work is needed to document this more fully.

Barrier islands are present intermittently along the southern coast of the Arabian Gulf, the most continuous set stretching for nearly 300 km along the United Arab Emirates (UAE) and adjacent coasts (Purser, 1973). This notwithstanding, how commonly barrier islands formed in the more extensive shallow carbonate ramp settings of the geological past (Burchette & Wright, 1992) is difficult to assess. Evidence of the presence of siliciclastic barriers is typically not well-preserved in transgressive sequences, as the mobile landforms continually erode on their seaward face and migrate landward, leaving only a coarse lag erosively overlying back-barrier lagoon sediments or older material (Boyd & Penland, 1981; Boyd, 2010). As with siliciclastic equivalents, evidence of the presence of mobile carbonate barrier systems having formed during transgressive periods may be challenging to recognize in the rock record due to similar sediment recycling, and the realization that no extensive karstification or exposure evidence will be preserved along most of the barrier's retreat path. In these areas, the only evidence of the former barrier will be the possible preservation of lagoonal deposits in topographic lows on the underlying surface. The thin, linear, discontinuous strands of beachrock providing evidence of recent barrier retreat at Al Ruwais would likely be difficult to recognize in the rock record. Other evidence may include the observed mixing of lagoonal and open-shelf skeletal assemblages in the transgressive lag, as has been noted in the cool-water realm (Rivers *et al.*, 2007), where barrier islands are more commonly observed. The only

locations where the actual barrier can be preserved is at the transgressive–regressive turnaround, or at rare places where the shoreface steps up and over the barrier, either because of very rapid sea-level rise or because the barrier stalls against a topographic step (Storms *et al.*, 2008).

Independent of preservation issues, Burchette & Wright (1992) noted that ramps were commonly the dominant carbonate platform type during geological ages when reef complexes were less common. Therefore if barrier island formation is inhibited by the presence of reefs, a greater presence of barrier islands in the past may correlate positively with times of ramp development. Another speculative reason that barrier island formation may be more common in ramp settings is ramp geometry, as the low gradient of the ramp margin is expected to provide the space during transgressive flooding in which laterally-extensive lagoons might be expected. The absence of carbonate barriers in modern shelf settings may reflect the absence of such lagoon accommodation. In areas with lithified rocks along the highstand coast that lack abundant sediment, a wave-cut notch is created at the highstand elevation (cf. Sisma-Ventura *et al.*, 2017, and references therein). The last several interglacial highstands have all risen to approximately the same elevation (Shackleton, 2000), and it is likely in tectonically stable areas that the current highstand has reoccupied an earlier notch. In such cases there is no space for the creation of a lagoon and, hence, barrier islands cannot exist. A survey of areas with carbonate beaches today using Google Earth® indicates that this situation is common, whereas areas with siliciclastic barrier islands generally lack such notches, perhaps because of the unconsolidated nature of previous highstand deposits, or have well-developed incised valleys in which lagoons can form.

Finally, with the exception of the early Triassic, geological times when ramp complexes were common (Burchette & Wright, 1992) were times of calcite seas (Sandberg, 1983), when early cementation associated with aragonite dissolution in meteoric waters would have been less common. In that way the aragonite-poor cool-water carbonate systems are analogues for calcite-sea carbonates (James, 1997), the greater presence of barrier island systems in the modern cool-water realm may well point to the same for the ramps of calcite seas. One example was reported by Wright (1986), where a Mississippian ramp sequence was interpreted to have been developed in response to the landward migration of a 'barrier' implied to have been an island (Wright, 1986, fig. 16). In summary, although direct evidence may be sparse, mobile carbonate barrier island systems are likely to have been more common in geological periods when ramp settings predominated due to restricted reef development, conducive platform geometry and limited early meteoric cementation.

Implications for subsurface models of greenhouse ramps

In the Al Ruwais area two temporally-distinct and spatially-distinct, and in some ways dissimilar, sets of coastal carbonate deposits formed over the past *ca* 7000 years. During the mid-Holocene (*ca* 7000 to 1400 years ago), a narrow barrier system with a muddy back-barrier lagoon fringed the shoreline, and a shoreline-parallel coral reef system flourished immediately in front of it. Approximately 1400 years ago, the depositional system was forced to form a new barrier *ca* 3 km to the north (Fig. 11) in response to an approximate 1·6 m sea-level fall, the exact timing and duration of which are uncertain. Assuming that deposition soon followed sediment formation, the age of back-barrier sediments overlying the coral deposits in core 5 indicates that the sea-level fall was sudden. The newly-established system lacks an extensive growing coral reef (some patch reefs formed seaward of the current barrier islands), and the back-barrier system is much wider and sandier than the mid-Holocene equivalent. Modern barrier island deposits at Al Ruwais are coarser-grained than deposits immediately behind and in front of the barrier (Purkis *et al.*, 2017). This was also likely true during the mid-Holocene, as the onshore barrier-beach grainstone deposits are coarser than those of the onshore back-barrier lagoon, where packstone-textured and wackestone-textured sediments are found. If it is presumed that primary porosity is a control on eventual fluid flow and storage capacity, it is important to point out that the mid-Holocene and modern barrier deposits are separated by *ca* 3 km of finer-grained carbonate sediment (Fig. 11), generating disconnected, shore-parallel, ribbon-shaped sand bodies. Some facies models of carbonate ramps imply that prograding 'barrier bank' bodies are continuous and connected (e.g. Read, 1985). This assumption might be particularly held for rocks deposited during greenhouse

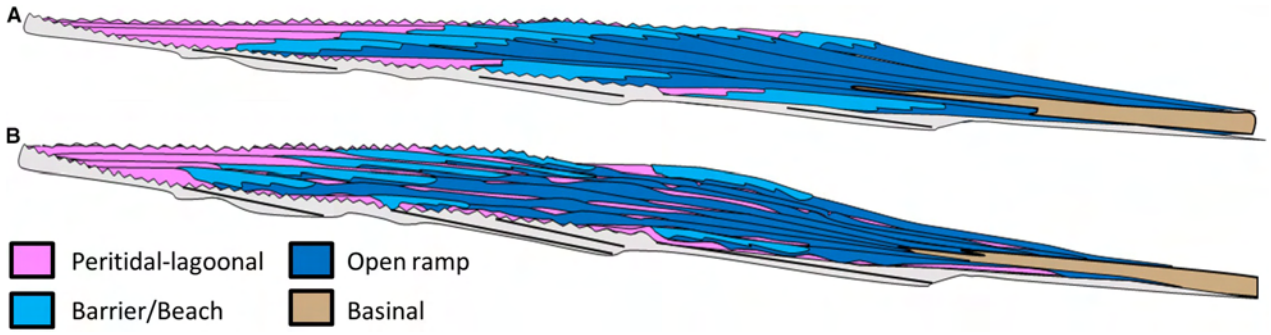

Fig. 13. Sequence stratigraphic models of ramp carbonates: (A) after Handford & Loucks (1993); and (B) based on expectations assuming mobile barrier island migration during transgression and strand plain progradation during highstand and regression.

times when sea-level changes are thought to have been lower amplitude relative to today's icehouse period. Read (1995) for instance maintains that during greenhouse times: "parasequences tend to have layer cake stacking patterns" and "grainstone facies show limited lateral migration from cycle to cycle". The amplitude of recent sea-level change at Al Ruwais (<2 m) and the length of time over which it likely occurred (a few thousand years), might be similar to that of high-order sea-level changes during greenhouse periods. For instance, in the Mesozoic metre-scale sea-level fluctuations are thought to have been common (Skelton, 2003), and sub-Milankovitch depositional cycles were produced over a period of only a few thousand years (Zühlke *et al.*, 2003). This is not to say that Read's (1985) generalizations about greenhouse depositional architecture were incorrect, but that the Al Ruwais situation offers an alternative model, where step-wise ramp progradation can occur over greenhouse-cycle-type periods and amplitudes creating grainstone bodies (barrier island deposits) that are separated spatially by significant areas of lower-energy deposits. The width and continuity of back-barrier facies belts is likely a function of the antecedent topography, with facies belts narrowing in areas of more steeply-dipping bedrock.

Sequence stratigraphic models of carbonate ramp deposits (e.g. Handford & Loucks, 1993; Kerans & Tinker, 1997; Schlager, 2005) perhaps reflect the understanding gained from observation of warm-water reefal systems common in the modern setting. The tenets of these models include: (i) the concept of a lag time (Tipper, 1997) between sea-level rise and carbonate grain production, caused by a slow-growth phase (Schlager, 2005) after exposure; (ii) the development, during times of relative sea-level stability, of a high-energy reef or grain body where normal wave base intersects the ramp, separating lower-energy 'back-barrier' facies from lower-energy open-marine deposits; and (iii) the generally-basinward stepping of all facies as carbonate production reaches full potential. These perceptions lend themselves to sequence stratigraphic models with the following characteristics (Fig. 13A): (i) progradation within a parasequence of both barrier *and* back-barrier deposits over open shelf deposits; (ii) broad segregation between back-barrier and open marine deposits; and (iii) the amalgamation of barrier deposits in highstand systems tracts.

Using analogues from the modern Qatar coastline, and integrating the understanding from siliciclastic studies of wave-dominated shorelines, Fig. 13B depicts an alternative sequence stratigraphic model for carbonate ramps forming in non-reefal settings. This model assumes that barrier islands nucleate during the initiation of transgression and keep up with sea-level rise, migrating landward across the ramp. Such an assumption is supported both by the apparent rapid formation of barrier islands at Al Ruwais in response to sea-level change, and the inferred presence of similar carbonate barriers required for the formation of saline waters (in protected lagoons) on the cool-water shelves of southern Australia during the Flandrian Transgression (Rivers *et al.*, 2009). The model also assumes that, during regressive phases, strand plain or chenier deposits similar to those observed along Qatar coasts south of Al Ruwais (Billeaud *et al.*, 2014; Strohmenger & Jameson, 2015) construct progradational shorelines. Applying these depositional motifs yields a stratigraphic model that

differs from the ramp model described above in three ways. First, parasequence bases both at the highstand shoreline, and in more basinward settings, variably include erosionally-truncated remnants of lagoonal deposits stranded by the passing of the barrier during transgression. Such deposits will preferentially occupy topographically low areas on the underlying parasequence (Fig. 13B). Second, highstand shoreline grainstones are typically not stacked and amalgamated barrier deposits, but are amalgamated shoreface deposits, or chenier bodies separated by fine-grained lagoonal deposits. Third, within the progradational phase of coastal carbonate parasequences, subtidal lagoons are not expected, as barrier islands required for their development are more common during transgressions (retrogradation). Deposits expected for progradational shorelines (strand plains and cheniers), will not be covered by prograding lagoonal deposits, as commonly depicted for ramp models (Fig. 13A), since there is no accommodation behind the shoreline. Lagoonal deposits overlying barrier deposits are predicted in the model but are associated with transgression over the barrier in the succeeding parasequence. This type of succession was interpreted by Wright (1986) for a Carboniferous carbonate ramp deposit in Wales.

CONCLUSIONS

The Al Ruwais area of northern Qatar has been the site of shallow water carbonate sedimentation since the mid-Holocene. Two distinct depositional packages have been identified. Between *ca* 7000 and 1400 years ago, when sea-level was up to 1·6 m higher than today, a barrier/back-barrier system was active in an area immediately landward of the modern shoreline. During the same period, a laterally-continuous coral reef flourished in the open waters *ca* 3 km to the north. Towards the end of this period sea-level fell to its current position, and the reefal system died, perhaps due to exposure or the influx of detrital sediment. Between 1400 and 800 years ago a new barrier island was established directly on top of the moribund reef, and the old barrier to the south was exposed to the meteoric realm. Over the past *ca* 800 years the new barrier has retreated landward as much as 1 km to its current position.

This study demonstrates that the processes forming mobile carbonate barrier island systems are identical to those that form siliciclastic equivalents. The paucity of modern carbonate barrier islands relative to siliciclastic analogues likely reflects the influence of reef structures and flat-topped platforms in dissipating wave energy before it reaches the shoreline, and early cementation in the carbonate realm which limits shoreline erosion to some (small) extent. Carbonate barrier islands appear to be more common in cool-water realms, where reefs are absent and early cementation is inhibited. For similar reasons, carbonate barrier islands were likely more common in warm-water settings during geological periods when ramp systems were dominant and calcite seas prevailed. Due to the self-cannibalizing nature of barrier island systems, however, evidence of their passage through a particular location along the shoreline-transit path is challenging to recognize in the rock record.

ACKNOWLEDGEMENTS

The authors would like to thank Sam Purkis for providing some images used in this publication. We are also indebted to Jeremy Jameson who oversaw the collection of four ^{14}C dates used for this publication during his tenure with EMRQ, and who generously introduced JRM and CJS to the field area. Dominik Brill and Dennis Wolf are acknowledged for their support during field work. We thank P. Wang for sharing his understanding of barrier island systems with RD. This report has been greatly improved by the helpful comments of two anonymous reviewers and by associate editor Stephen Lokier.

REFERENCES

Aagaard, T., **Davidson-Arnott, R.**, **Greenwood, B.** and **Nielsen, J.** (2004) Sediment supply from shoreface to dunes: linking sediment transport measurements and long-term morphological evolution. *Geomorphology*, **60**, 205–224.

Ahr, W.M. (1973) The carbonate ramp: an alternative to the shelf model. *Trans. Gulf Coast Ass. Geol. Soc.*, **23**, 221–225.

Alothman, A.O., **Bos, M.S.**, **Fernandes, R.M.S.** and **Ayhan, E.M.** (2014) Sea level rise in the north-western part of the Arabian Gulf. *J. Geodyn.*, **81**, 105–110.

Alsharhan, A.S. and **Kendall, C.G.St.C.** (2003) Holocene coastal carbonates and evaporites of the southern Arabian Gulf and their ancient analogues. *Earth Sci. Rev.*, **61**, 191–243.

Al-Yousef, M. (2003) *Mineralogy, geochemistry and origin of Quaternary Sabkhas in the Qatar Peninsula, Arabian Gulf*. Unpublished PhD thesis, University of Southampton, Southampton, 248 pp.

Backstrom, J.T., **Jackson, D.W.T.** and **Cooper, J.A.G.** (2009) Mesoscale shoreface morphodynamics on a high-energy regressive coast. *Cont. Shelf Res.*, **29**, 1361–1372.

Barwis, J. and **Hayes, M.** (1979) Regional patterns of modern barrier island and tidal inlet deposits as applied to paleoenvironmental studies. In: *Carboniferous Depositional Environments in the Appalachian Region: Columbia, South Carolina, Carolina Coal Group* (Eds J.C. Ferm and J.C. Horne), pp. 472–508. Carolina Coal Group, University of South Carolina, Columbia.

Billeaud, I., **Caline, B.**, **Livas, B.**, **Tessier, B.**, **Davaud, E.**, **Frebourg, G.**, **Hasler, C.-A.**, **Laurier, D.** and **Pabian-Goyheneche, C.** (2014) The carbonate-evaporite lagoon of Al Dakhirah (Qatar): an example of a modern depositional model controlled by longshore transport. In: *Sedimentary Coastal Zones from High to Low Latitudes: Similarities and Differences* (Eds I.P. Martini and H.R. Wanless) Geological Society, London, Special Publications, **388**, 561–588.

Boyd, R. (2010) Transgressive wave-dominated coasts. In: *Facies Models 4* (Eds N.P. James and R.W. Dalrymple) Geotext 6, pp. 265–294. Geological Association of Canada, St. John's.

Boyd, R. and **Penland, S.** (1981) Washover of Deltaic Barriers on Louisiana Coast. *Trans. Gulf Coast Assoc. Geol. Soc.*, **31**, 243–248.

Brill, D., **May, S.M.**, **Engel, M.**, **Reyes, M.**, **Pint, A.**, **Opitz, S.**, **Dierick, M.**, **Gonzalo, L.A.**, **Esser, S.** and **Brückner, H.** (2016) Typhoon Haiyan's sedimentary record in coastal environments of the Philippines and its palaeotempestological implications. *Nat. Hazard. Earth Syst. Sci.*, **16**, 2799–2822.

Burchette, T.P. and **Wright, V.P.** (1992) Carbonate ramp depositional systems. *Sed. Geol.*, **79**, 3–57.

Calvet, F., **Tucker, M.** and **Henton, J.** (1990) Middle Triassic carbonate ramp systems in the Catalan Basin, northeast Spain. facies, systems tracts, sequences and controls. In: *Carbonate Platforms, Facies, Sequences and Evolution* (Eds M.E. Tucker, J.L. Wilson, P.D. Crevello, J.R. Sarg and J.F. Read), International Association of Sedimentologists, Special Publication, **9**, 79–108.

Cooper, J., **Jackson, D.**, **Dawson, A.**, **Dawson, S.**, **Bates, C.** and **Ritchie, W.** (2012) Barrier islands on bedrock: a new landform type demonstrating the role of antecedent topography on barrier form and evolution. *Geology*, **40**, 923–926.

Cowell, P.J., **Roy, P.S.**, **Cleveringa, J.** and **De Boer, P.L.** (1999) Simulating coastal systems tracts using the shoreface translation model. In: *Numerical Experiments in Stratigraphy: Recent Advances in Stratigraphic and Sedimentologic Computer Simulations* (Eds J.W. Harbaugh, W.L. Watney, E.C. Rankey, R. Slingerland, R.H. Goldstein and E.K. Franseen) Society of Economic Paleontologists and Mineralogists, Special Publication, **62**, 165–175.

Dalrymple, R.W. (2010) Tidal depositional systems. In: *Facies Models 4* (Eds N.P. James and R.W. Dalrymple) Geotext 6, pp. 201–232. Geological Association of Canada, St. John's.

Dalrymple, R.W., **Zaitlin, B.A.** and **Boyd, R.** (1992) Estuarine facies models; conceptual basis and stratigraphic implications. *J. Sed. Res.*, **62**, 1130–1146.

Davies, J. (1964) A morphogenetic approach to world shorelines. *Z. Geomorphol.*, **8**, 127–144.

Davis, R.A. (1985) Beach and nearshore zone. In: *Coastal Sedimentary Environments* (Ed. R.A. Davis), pp. 379–444. Springer, New York.

Davis, R.A. (1994) Barrier island systems—a geologic overview. In: *Geology of Holocene Barrier Island Systems* (Ed. R.A. Davis), pp. 1–46. Springer-Verlag, Berlin.

Davis, R.A., **FitzGerald, D.M.** and **Duncan, M.** (2004) *Beaches and Coasts*. Blackwell Publishing, Malden, 419 pp.

De Beaumont, L. (1845) *Leçon de Géologie Practique. Septieme Leçon*. Bertrand, Paris, pp. 221–252

Desruelles, S., **Fouache, É.**, **Ciner, A.**, **Dalongeville, R.**, **Pavlopoulos, K.**, **Kosun, E.**, **Coquinot, Y.** and **Potdevin, J.L.** (2009) Beachrocks and sea level changes since Middle Holocene: comparison between the insular group of Mykonos–Delos–Rhenia (Cyclades, Greece) and the southern coast of Turkey. *Global Planet. Change*, **66**, 19–33.

Dewey, J.F., **Pitman, W.C.**, **Ryan, W.B.** and **Bonnin, J.** (1973) Plate tectonics and the evolution of the Alpine system. *Geol. Soc. Am. Bull.*, **84**, 3137–3180.

Dougherty, A.J. (2018) Prograded coastal barriers provide paleoenvironmental records of storms and sea level during late Quaternary highstands. *J. Quat. Sci.*, **33**, 501–517.

Dunham, R.J. (1962) Classification of carbonate rocks according to depositional textures. In: *Classification of Carbonate Rocks – A Symposium* (Ed. W.E. Ham), American Association of Petroleum Geologists Memoir, **1**, 108–121.

Eccleston, B., **Pike, J.** and **Harhash, I.** (1981) *The Water Resources of Qatar and their Development, Volumes I-III: United Nations Food and Agricultural Organization, Technical Report No. 5, Doha, Qatar.* Agricultural Development Project, Doha, 390, pp.

El-Sabh, M. and **Murty, T.** (1989) Storm surges in the Arabian Gulf. *Nat. Hazards*, **1**, 371–385.

Engel, M. and **Brückner, H.** (2014) The South Qatar Survey Project (SQSP) - Preliminary findings on Holocene coastal changes and geoarchaeological archives. *Z. Orient-Archäol.*, **7**, 290–301.

Fairbridge, R.W. (1961) Eustatic changes in sea level. *Phys. Chem. Earth*, **4**, 99–185.

Fleming, R.H. and **Revelle, R.** (1955) Physical processes in the ocean. In: *Recent Marine Sediments* (Ed. P.D. Trask), SEPM Special Publication, **4**, 48–141.

Flemming, B.W. (2012) Siliciclastic back-barrier tidal flats. In: *Principles of Tidal Sedimentology* (Eds R.A. Davis and R.W. Dalrymple), pp. 231–267. Springer, Dordrecht.

Fruergaard, M., **Andersen, T.J.**, **Nielsen, L.H.**, **Johannessen, P.N.**, **Aagaard, T.** and **Pejrup, M.** (2015a) High-resolution reconstruction of a coastal barrier system: impact of Holocene sea-level change. *Sedimentology*, **62**, 928–969.

Fruergaard, M., **Møller, I.**, **Johannessen, P.N.**, **Nielsen, L.H.**, **Andersen, T.J.**, **Nielsen, L.**, **Sander, L.** and **Pejrup, M.** (2015b) Stratigraphy, evolution, and controls of a Holocene transgressive–regressive barrier island under changing sea level: Danish North Sea coast. *J. Sed. Res.*, **85**, 820–844.

Fruergaard, M., **Johannessen, P.N.**, **Nielsen, L.H.**, **Nielsen, L.**, **Møller, I.**, **Andersen, T.J.**, **Piasecki, S.** and **Pejrup, M.** (2018) Sedimentary architecture and depositional controls of a Holocene wave-dominated barrier-island system. *Sedimentology*, **65**, 1170–1212.

Gilbert, G.K. (1885) The topographic features of lake shores. US Geological Survey, 5th Annual Report, pp. 69–123.

Ginsburg, R.N. and **James, N.P.** (1974) Holocene carbonate sediments of continental shelves. In: *The Geology of Continental Margins* (Eds C.A. Burk and C.L. Drake), pp. 137–155. Springer-Verlag, New York.

Glennie, K.W. (2005) *The Desert of Southeast Arabia: Desert Environments and Sediments*. Gulf PetroLink Publishers, Bahrain, 213 pp.

Glennie, K., **Clarke, M.H.**, **Boeuf, M.**, **Pilaar, W.** and **Reinhardt, B.** (1990) Inter-relationship of Makran-Oman Mountains belts of convergence. In: *The Geology and Tectonics of the Oman Region* (Eds A.F.H. Robertson, M.P. Searle and A.C. Ries) Geological Society London, Special Publications, **49**, 773–786.

Handford, C.R. and **Loucks, R.G.** (1993) Carbonate depositional sequences and systems tracts—responses of carbonate platforms to relative sea-level changes. In: *Carbonate Sequence Stratigraphy: Recent Developments and Applications* (Eds R.G. Loucks and J.F. Sarg), AAPG Memoir, **57**, 3–42.

Harris, P.M., **Purkis, S.J.** and **Ellis, J.** (2011) Analyzing spatial patterns in modern carbonate sand bodies from Great Bahama Bank. *J. Sed. Res.*, **81**, 185–206.

Hayes, M. (1979) Barrier island morphology as a function of tidal and wave regime. In: *Barrier Islands* (Ed. S.P. Leatherman), pp. 1–27. Academic, New York.

James, N.P. (1997) The cool-water carbonate depositional realm. In: *Cool-Water Carbonates* (Eds N.P. James and J.A.D. Clarke) The Society of Economic Paleontologists and Mineralogists, Special Publication, **56**, 1–22.

James, N.P. and **Bone, Y.** (2017) Quaternary aeolianites in south-east Australia–a conceptual linkage between marine source and terrestrial deposition. *Sedimentology*, **64**, 1005–1043.

James, N.P. and **Choquette, P.W.** (1990a) Limestones–seafloor diagenetic environments. In: *Diagenesis* (Eds I.A. McIlreath and W. Morrow) Reprint Series 4, pp. 13–34. Geoscience Canada, Ottawa.

James, N.P. and **Choquette, P.W.** (1990b) Limestones—the burial diagenetic environment. In: *Diagenesis* (Eds I.A. McIlreath and W. Morrow) Reprint Series 4, pp. 35–74. Geoscience Canada, Ottawa.

James, N.P. and **Macintyre, I.G.** (1985) Carbonate depositional environments, modern and ancient. Part 1. Reefs: zonation, depositional facies, diagenesis. *Colorado Sch. Min. Q.*, **80**, 1–70.

Jones, B. (2010) Warm-water Neritic Carbonates. In: *Facies Models 4* (Eds N.P. James and R.W. Dalrymple) Geotext 6, pp. 341–370. Geological Association of Canada, St. John's.

Joury, M.R.F., **James, N.P.** and **James, C.** (2018) Nearshore cool-water carbonate sedimentation and provenance of Holocene calcareous strandline dunes, southeastern Australia. *Aust. J. Earth Sci.*, **65**, 221–242.

Kämpf, J. and **Sadrinasab, M.** (2005) The circulation of the Persian Gulf: a numerical study. *Ocean Sci.*, **2**, 27–41.

Kassler, P. (1973) The structural and geomorphic evolution of the Persian Gulf. In: *The Persian Gulf* (Ed. B.H. Purser), pp. 11–32. Springer, Berlin.

Kelletat, D. (2006) Beachrock as sea-level indicator? Remarks from a geomorphological point of view. *J. Coastal Res.*, **22**, 1558–1564.

Kerans, C. and **Kempter, K.A.** (2002) Hierarchical stratigraphic analysis of a carbonate platform, Permian of the Guadalupe Mountains. AAPG Datapages Discovery Series 5 CD ROM.

Kerans, C. and **Tinker, S.W.** (1997) Sequence Stratigraphy and Characterization of Carbonate Reservoirs. SEPM Short Course Notes 40, 130 pp.

Kinsela, M.A., **Daley, M.J.** and **Cowell, P.J.** (2016) Origins of Holocene coastal strandplains in Southeast Australia: Shoreface sand supply driven by disequilibrium morphology. *Mar. Geol.*, **374**, 14–30.

Lambeck, K. (1996) Shoreline reconstructions for the Persian Gulf since the last glacial maximum. *Earth Planet. Sci. Lett.*, **142**, 43–57.

Logan, B.W., **Harding, J.L.**, **Ahr, W.M.**, **Williams, J.D.** and **Snead, R.G.** (1969) Carbonate sediments and reefs, Yucatan Shelf, Mexico. *Am. Assoc. Pet. Geol. Mem.*, **11**, 1–98.

Lokier, S.W., **Bateman, M.D.**, **Larkin, N.R.**, **Rye, P.** and **Stewart, J.R.** (2015) Late Quaternary sea-level changes of the Persian Gulf. *Quatern. Res.*, **84**, 69–81.

Loughland, R.A., **Al-Abdulkader, K.A.**, **Wyllie, A.** and **Burwell, B.O.** (2012) Anthropogenic induced geomorphological change along the Western Arabian Gulf coast. In: *Studies on Environmental and Applied Geomorphology* (Eds T. Piacentini and E. Miccadei), pp. 194–218. InTech, Croatia.

Marzouk, I. and **El Sattar, M.** (1994) Wrench tectonics in Abu Dhabi, United Arab Emirates. In: *Middle East Petroleum Geosciences* (Ed. M.I. Al-Husseini), GeoArabia, **1**, 655–668.

Mauz, B., **Vacchi, M.**, **Green, A.**, **Hoffmann, G.** and **Cooper, A.** (2015) Beachrock: a tool for reconstructing relative sea level in the far-field. *Mar. Geol.*, **362**, 1–16.

McGee, W.D. (1890) Encroachments of the sea. *Forum*, **9**, 437–449.

McKee, E.D. and **Ward, W.C.** (1983) Eolian environment. In: *Carbonate Depositional Environments* (Eds R.A. Scholle, D.G. Bebout and C.H. Moore) American Association of Petroleum Geologists, Memoir, **33**, 131–170.

Mitrovica, J. and **Milne, G.** (2002) On the origin of late Holocene sea-level highstands within equatorial ocean basins. *Quatern. Sci. Rev.*, **21**, 2179–2190.

Neumann, A.C. and **Macintyre, I.** (1985) Reef response to sea-level rise: keep-up, catch-up, or give-up. In: *Proceedings of the Fifth International Coral Reef Congress, Tahiti* (Eds C. Gabrie, J.L. Toffart and B. Salvat) International Society for Reef Studies, **3**, 105–110.

Niedoroda, A.W., **Swift, D.J.**, **Hopkins, T.S.** and **Ma, C.-M.** (1984) Shoreface morphodynamics on wave-dominated coasts. *Mar. Geol.*, **60**, 331–354.

Oliver, T.S., **Donaldson, P.**, **Sharples, C.**, **Roach, M.** and **Woodroffe, C.D.** (2017a) Punctuated progradation of the Seven Mile Beach Holocene barrier system, southeastern Tasmania. *Mar. Geol.*, **386**, 76–87.

Oliver, T., **Tamura, T.**, **Hudson, J.** and **Woodroffe, C.D.** (2017b) Integrating millennial and interdecadal shoreline changes: Morpho-sedimentary investigation of two prograded barriers in southeastern Australia. *Geomorphology*, **288**, 129–147.

Phleger, F.B. and **Ayala-Castanares, A.** (1971) Processes and history of Terminos lagoon, Mexico. *Am. Assoc. Petrol. Geol. Bull.*, **55**, 2130–2140.

Pilkey, O.H. and **Fraser, M.E.** (2003) *A Celebration of the World's Barrier Islands*. Columbia University Press, New York, 400 pp.

Plint, A.G. (2010) Wave- and Storm-Dominated Shoreline and Shallow Marine Systems. In: *Facies Models 4* (Eds N.P. James and R.W. Dalrymple) Geotext 6, pp. 265–294. Geological Association of Canada, St. John's.

Purkis, S., **Rivers, J.**, **Strohmenger, C.J.**, **Warren, C.**, **Yousif, R.**, **Ramirez, L.** and **Riegl, B.** (2017) Complex interplay

between depositional and petrophysical environments in Holocene tidal carbonates (Al Ruwais, Qatar). *Sedimentology*, **64**, 1646–1675.

Purser, B.H. (1973) *The Persian Gulf: Holocene Carbonate Sedimentation and Diagenesis in a Shallow Epicontinental Sea*. Springer-Verlag, New York, 471 pp.

Purser, B.H. and **Evans, G.** (1973) Regional sedimentation along the Trucial coast, SE Persian Gulf. In: *The Persian Gulf: Holocene Carbonate Sedimentation and Diagenesis in a Shallow Epicontinental Sea* (Ed. B.H. Purser), pp. 211–231. Springer, New York.

Raff, J.L., **Shawler, J.L.**, **Ciarletta, D.J.**, **Hein, E.A.**, **Lorenzo-Trueba, J.** and **Hein, C.J.** (2018) Insights into barrier-island stability derived from transgressive/regressive state changes of Parramore Island, Virginia. *Mar. Geol.*, **403**, 1–19.

Read, J.F. (1985) Carbonate platform facies models. *Am. Assoc. Petrol. Geol. Bull.*, **69**, 1–21.

Read, J.F. (1995) Overview of carbonate platform sequences, cycle stratigraphy and reservoirs in greenhouse and ice-house worlds. In: *Milankovitch Sea-level Changes, Cycles, and Reservoirs on Carbonate Platforms in Greenhouse and Ice-house Worlds* (Eds J.F. Read, C. Kerans, L.J. Webber, J.F. Sarg and F.M. Wright), SEPM Short Course, **35**, 1–102.

Reimer, P.J., **Bard, E.**, **Bayliss, A.**, **Beck, J.W.**, **Blackwell, P.G.**, **Bronk Ramsey, C.**, **Buck, C.E.**, **Cheng, H.**, **Edwards, R.L.**, **Friedrich, M.**, **Grootes, P.M.**, **Guilderson, T.P.**, **Haflidason, H.**, **Hajdas, I.**, **Hatté, C.**, **Heaton, T.J.**, **Hoffmann, D.L.**, **Hogg, A.G.**, **Hughen, K.A.**, **Kaiser, K.F.**, **Kromer, B.**, **Manning, S.W.**, **Niu, M.**, **Reimer, R.W.**, **Richards, D.A.**, **Scott, E.M.**, **Southon, J.R.**, **Staff, R.A.**, **Turney, C.S.M.** and **van der Plicht, J.** (2013) IntCal13 and Marine13 radiocarbon age calibration curves 0–50,000 years cal BP. *Radiocarbon*, **55**, 1869–1887.

Reynaud, J.Y. and **Dalrymple, R.W.** (2012) Shallow-marine tidal deposits. In: *Principles of Tidal Sedimentology* (Eds R.A. Davis Jr and R.W. Dalrymple), pp. 335–369. Springer, Berlin.

Rivers, J.M., **James, N.P.** and **Kyser, T.K.** (2007) Genesis of palimpsest cool-water carbonate sediment on the southern Australian margin. *J. Sed. Res.*, **77**, 480–494.

Rivers, J.M., **Kyser, T.K.** and **James, N.P.** (2009) Isotopic composition of a large benthic foraminifer: evidence for hypersaline environments across the Great Australian Bight during the Late Pleistocene. *Sed. Geol.*, **213**, 113–120.

Sandberg, P.A. (1983) An oscillating trend in Phanerozoic non-skeletal carbonate mineralogy. *Nature*, **305**, 19.

Sarnthein, M. (1972) Sediments and history of the postglacial transgression in the Persian Gulf and northwest Gulf of Oman. *Mar. Geol.*, **12**, 245–266.

Schlager, W. (2005) Carbonate Sedimentology and Sequence Stratigraphy. *SEPM Concepts Sed. Paleontol.*, **8**, 200.

Scholle, P.A. and **Ulmer-Scholle, D.S.** (2003) A color guide to the petrography of carbonate rocks: grains, textures, porosity, diagenesis. *Am. Assoc. Petrol. Geol. Mem.*, **77**, 486.

Schwartz, R.K. (1982) Bedform and stratification characteristics of some modern small-scale washover sand bodies. *Sedimentology*, **29**, 835–849.

Seyedmehdi, Z., **George, A.D.** and **Tucker, M.E.** (2016) Sequence development of a latest Devonian-Tournaisian distally-steepened mixed carbonate–siliciclastic ramp, Canning Basin, Australia. *Sed. Geol.*, **333**, 164–183.

Shackleton, N.J. (2000) The 100,000-year ice-age cycle identified and found to lag temperature, carbon dioxide, and orbital eccentricity. *Science*, **289**, 1897–1902.

Sheppard, C., **Al-Husiani, M.**, **Al-Jamali, F.**, **Al-Yamani, F.**, **Baldwin, R.**, **Bishop, J.**, **Benzoni, F.**, **Dutrieux, E.**, **Dulvy, N.K.** and **Durvasula, S.R.V.** (2010) The Gulf: a young sea in decline. *Mar. Pollut. Bull.*, **60**, 13–38.

Sisma-Ventura, G., **Sivan, D.**, **Shtienberg, G.**, **Bialik, O.M.**, **Filin, S.** and **Greenbaum, N.** (2017) Last interglacial sea level high-stand deduced from well-preserved abrasive notches exposed on the Galilee coast of northern Israel. *Palaeogeogr. Palaeoclimatol. Palaeoecol.*, **470**, 1–10.

Skelton, P.W. (2003) Fluctuating sea-level. In: *The Cretaceous World* (Ed. P.W. Skelton) pp. 67–84. The Open University, Cambridge University Press, Cambridge.

Southon, J., **Kashgarian, M.**, **Fontugne, M.**, **Metivier, B.** and **Yim, W.W.** (2002) Marine reservoir corrections for the Indian Ocean and Southeast Asia. *Radiocarbon*, **44**, 167–180.

Storms, J.E.A. (2003) Event-based stratigraphic simulation of wave-dominated shallow-marine environments. *Mar. Geol.*, **199**, 83–100.

Storms, J.E.A., **Weltje, G.J.**, **Terra, G.J.**, **Cattaneo, A.** and **Trincardi, F.** (2008) Coastal dynamics under conditions of rapid sea-level rise: Late Pleistocene to Early Holocene evolution of barrier– lagoon systems on the northern Adriatic shelf (Italy). *Quat. Sci. Rev.*, **27**, 1107–1123.

Strohmenger, C.J. and **Jameson, J.** (2015) Modern coastal systems of Qatar as analogues for arid climate carbonate reservoirs: improving geological and reservoir modelling. *First Break*, **33**, 41–50.

Strohmenger, C.J., **Shebl, H.**, **Al-Mansoori, A.**, **Al-Mehsin, K.**, **Al-Jeelani, O.**, **Al-Hosani, I.**, **Al-Shamry, A.** and **Al-Baker, S.** (2010) Facies stacking patterns in a modern arid environment: a case study of the Abu Dhabi sabkha in the vicinity of Al-Qanatir Island, United Arab Emirates. In: *Quaternary Carbonate and Evaporite Sedimentary Facies and Their Ancient Analogs* (Eds A.S. Alsharhan and C.G.St.C. Kendall) International Association of Sedimentologists, Special Publication, **43**, 149–182.

Stutz, M.L. and **Pilkey, O.H.** (2001) A review of global barrier island distribution. *J. Coastal Res.*, **34**, 15–22.

Swift, D.J.P. (1975) Barrier-island genesis: evidence from the central Atlantic shelf, eastern USA. *Sed. Geol.*, **14**, 1–43.

Tipper, J.C. (1997) Modeling carbonate platform sedimentation—lag comes naturally. *Geology*, **25**, 495–498.

Tucker, M.E. (1991) Sequence stratigraphy of carbonate-evaporite basins: models and application to the Upper Permian (Zechstein) of northeast England and adjoining North Sea. *J. Geol. Soc. London*, **148**, 1019–1036.

Tucker, M.E. and **Wright, V.P.** (1990) *Carbonate Sedimentology*. Blackwell Scientific, Oxford, 482 pp.

Vousdoukas, M.I., **Velegrakis, A.F.** and **Plomaritis, T.A.** (2007) Beachrock occurrence, characteristics, formation mechanisms and impacts. *Earth Sci. Rev.*, **85**, 23–46.

Walkden, G. and **Williams, A.** (1998) Carbonate ramps and the Pleistocene-Recent depositional systems of the Arabian Gulf. In: *Carbonate Ramps* (Eds V.R. Wright and T.R. Burchette) Geological Society of London, Special Publications, **149**, 43–53.

Webb, G.E., **Jell, J.S.** and **Baker, J.C.** (1999) Cryptic intertidal microbialites in beachrock, Heron Island, Great Barrier Reef: implications for the origin of microcrystalline beachrock cement. *Sed. Geol.*, **126**, 317–334.

Wright, V.P. (1986) Facies sequences on a carbonate ramp: the Carboniferous Limestone of South Wales. *Sedimentology*, **33**, 221–241.

Yousif, R., **Warren, C.**, **Ben-Hamadou, R.** and **Husrevoglu, S.** (2018) Modeling sediment transport in Qatar: application for coastal development planning. *Integr. Environ. Assess. Manag.*, **14**, 240–251.

Yu, Y., **Notaro, M.**, **Kalashnikova, O.V.** and **Garay, M.J.** (2016) Climatology of summer Shamal wind in the Middle East. *J. Geophys. Res. Atmos.*, **121**, 289–305.

Zaremba, N., **Mallinson, D.J.**, **Leorri, E.**, **Culver, S.**, **Riggs, S.**, **Mulligan, R.**, **Horsman, E.** and **Mitra, S.** (2016) Controls on the stratigraphic framework and paleoenvironmental change within a Holocene estuarine system: Pamlico Sound, North Carolina, USA. *Mar. Geol.*, **379**, 109–123.

Zühlke, R., **Bechstädt, T.** and **Mundil, R.** (2003) Sub-Milankovitch and Milankovitch forcing on a model Mesozoic carbonate platform–the Latemar (Middle Triassic, Italy). *Terra Nova*, **15**, 69–80.

Manuscript received 4 October 2018; revision accepted 5 August 2019